RGNZ/MGPB

Springs of Variable Stiffness in the Control of Seismic Actions in Buildings

Rudarsko-geološko-naftni zbornik
(The Mining-Geology-Petroleum Engineering Bulletin)
UDC: 624.078.5-026.564:[624.042.7:519.6]
DOI: 10.17794/rgn.2023.2.2

Original scientific paper

Alexandre Wahrhaftig[1,3], Julia Dantas[2], Cibele Menezes[3], Larysa Neduzha[4]

[1] *Federal University of Bahia, Polytechnic School, Department of Construction and Structures, Rua Aristides Novis, 02, 5° andar, Federação, Salvador – BA, ZIP Code: 40210-630, Brazil, ORCID 0000-0002-7144-1917*

[2] *Federal University of Bahia, Polytechnic School, Researcher of the Institutional Scientific Initiation Program (PIBIC/UFBA-CNPq), Rua Aristides Novis, 02, 5° andar, Federação, Salvador – BA, ZIP Code: 40210-630, Brazil, ORCID 0000-0002-2520-3176*

[3] *Federal University of Bahia, Polytechnic School, Graduate Program in Civil Engineering, Rua Aristides Novis Street, 02, 8° andar, Federação, Salvador – BA, Brazil, ZIP Code: 40210-630, ORCID 0000-0002-3559-1803*

[4] *Ukrainian State University of Science and Technologies, Department of Theoretical and Structural Mechanics, Dnipro, Ukraine, 49010, ORCID 0000-0002-7038-3006*

Abstract

Many regions in the world have experienced the presence of intensive geological events. Given this reality, the control of vibrations caused by earthquakes on buildings is one of the great challenges in seismic regions, as they can cause structural, material, and personal damage, and must be considered with special attention when carrying out a structural project. For this reason, it is necessary to minimize the deleterious effects caused by earthquakes on buildings. In this sense, the present study seeks to evaluate, through the theory of mechanical vibrations, the use of springs of variable stiffness in the control of accelerations induced by seismic action, because springs introduce restoring forces in the system. The evaluation is done through numerical-computational simulation using the finite element method. The frame structure of an idealized building is used in the modelling, where columns and beams are represented by linear elements and the floors by shell elements. In the simulation, springs of variable stiffness are inserted into the joints to control the vibrations produced by earthquakes. These devices are added to the structural system at different heights and directions, aiming to keep the structure's behaviour unchanged, neutralizing the effects of the earthquake. Based on the obtained results, it is possible to verify the required stiffness and the position in which the springs must be inserted to obtain the constancy of the structural frequency of vibration during the earthquake action.

Keywords:
spring supports; variable stiffness; seismic action; computational simulation; structural vibrations

1. Introduction

During the elaboration of structural projects of buildings, an important parameter to consider is the effect of vibrations from dynamic loads, such as winds (**Wahrhaftig and Silva, 2017**; **Davenport, 1961**), seismic shocks and their effects (**Jaya Syahbana et al., 2021; Van Loon et al. 2020**), sound waves (**Rose et. al., 2006; Krylov, 1995**), and blast waves (**Yari et al., 2022; Smith et al. 1999**). The damage caused by the energy transferred by this type of force can seriously compromise the integrity of structures and foundations, in addition to causing irreparable human damage. The effects of earthquakes, caused by the movement of tectonic plates, generate large-scale damage to society, such as the destruction of cities, affecting the entire economy of the afflicted places. In addition, this phenomenon has also caused a considerable number of deaths around the world. Because they are natural disasters, they are part of uncontrollable scenarios, and so the structures of the buildings must be prepared to resist these events, minimizing their effects. In this regard interpreted seismic data is an important aspect of the process (**García et al., 2018**).

In this context, the study of vibration control has been deepened by several engineers around the world, who seek to prepare the physical infrastructure of society to support or live with the extreme events of nature. In this sense, vibration attenuators have been used as a successful control tool. However, seismic vibration attenuation devices can be costly and are poorly used in underdeveloped countries. For this reason, the present study seeks to evaluate the theoretical implementation of a simpler type of vibration control device, with variable stiffness, which may become an economical alternative for economically less favoured localities, but is also subject to seismic actions, commonly referred to by earthquakes.

According to **Bosse (2017)**, structures that present a good dynamic response to vibrations of any nature must

Corresponding author: Alexandre Wahrhaftig
e-mail address: alixa@ufba.br

have the necessary flexibility to cushion the displacements of the imposed movements and, simultaneously, the sufficient rigidity to withstand the remaining stresses of the other loads that are part of their working conditions. Also, according to that author, currently, most of the constructions have a low resistance to the effects of vibrations induced by various sources, mainly due to the widespread use of inflexible materials and prefabricated parts that have articulated bindings that favour gantry bonds with insufficient stiffness. Thus, vibration control gains space to reduce the risk of the collapse of buildings. In that context, **Wu et al. (2021)** affirm that the stiffness of frame structures is an essential mechanism to adjust the response of the structure under earthquake.

According to **Campos et al. (2016)**, neotectonics consist of the activity of moving tectonic plates in the region capable of reactivating the geological structures generated by the last recent large-scale tectonic event. Contributing to this event is the existing stress on the geomechanics surface (**Moomivand et al., 2022**). Particularly, in their study, **Preve et al. (2017)** state that the tremors that happen in Brazil have occurred mainly due to neotectonic failures. He conducted an overview of the regional neotectonic characteristics of the Brazilian continental shelf and showed that Brazil has 48 faults, with predominance in the Southeast and Northeast regions, then in the North and Midwest regions, and in smaller numbers in the South.

Tavares et al. (2013) mention the lack of dissemination of knowledge about seismic shocks in Brazil, an aspect that causes a lack of awareness of society, resulting in unpreparedness in the face of the occurrence of these events. According to **Seeber and Armbruster (1988)**, intraplate seismic shocks, if they have magnitude and depth equal to those of the plate edge, are the most dangerous for structural engineering. Therefore, studies aimed at the development of technologies capable of making structures resistant to seismic shocks are extremely relevant (in Brazil) because it is essential to prepare in cases of future geological disasters.

Thus, the relevance of the theoretical aspects present in this work is evidenced, even if synthetically. Therefore, seeking to mitigate the deleterious effects of seismic actions on buildings, a numerical-computational modelling elaborated through the finite element method (FEM) is performed to evaluate the use of springs, or analogous devices, of variable stiffness, to compensate possible vibration caused by seismic shocks in buildings, keeping the initial building design condition unchanged, or even, if not unchanged, leaving the current condition as close to its original one as possible.

It is noteworthy that springs are already commercially manufactured devices in a wide variety of stiffnesses and that there are many types of mechanisms that meet the described function, including those of a hydraulic nature, which are also widely used in the industry and construction, such as hydraulic jacks. Hydraulic jacks, including those of variable stiffnesses, have already been evaluated by **Mirfakhraei et al. (2019)** as an efficient control device to mitigate building displacements under seismic action.

2. Vibration Control Systems

In the field of buildings, **Gómez (2007)** reports that the advancement of executive techniques has allowed the construction of increasingly tall and slender structures, making them more subject to vibrations from wind, earthquakes, heavy traffic, and other dynamic loads present in the everyday life of society. Seeking to mitigate the effects of these actions, vibration control may be a viable option.

Studies on vibration control have been associated with the use of mechanical devices capable of acting on the dynamic properties of the system to be controlled. These devices have their components represented by springs and shock absorbers that make up the equation of the movement of the system and whose solution can be obtained by different pathways and methods. In the work of **Zhang et al. (2009)**, for example, numerical and analytical methods were used to evaluate the reduction of force to be transmitted in the resonance range of a simple mass-spring system. The efficacy of attenuation in this study was made by comparing one system with nonlinear springs to another with shock absorbers, also nonlinear. The results indicated that the springs were not able to withstand amplitude peaks with increasing vibration frequency but were effective in decreasing the induced vibration frequencies.

In the work developed by **Valencia et al. (2022)**, the attenuation of seismic effects was studied from the numerical-computational modelling of three flat-structure buildings. The buildings were excited by four different time functions representative of different seismic actions. The attenuation device used was based on fluid dampers and was positioned on different floors of the study buildings. The results were evaluated in terms of displacements, accelerations, and forces, and proved that the use of shock absorbers was positive in attenuating the responses of buildings. In a particular context, **Ikeda (2009)** surveyed buildings in Japan, a country known for its high seismic activity, and its different methods of vibration control, focusing on practical applications. The processes analysed by **Ikeda (2009)** were the mechanisms of tuned mass damping, whether active, passive, or semi-active. It is worth mentioning that passive systems are the most common and the simplest due to the ease of execution and design. It is very indicated when one knows or can predict the vibrations to which the structure will be subjected since it works in a certain vibration zone. Passive control mechanisms are normally performed with the aid of external devices capable of changing the stiffness and damping of the structure.

One of the best-known passive control systems is the tuned mass damper (TMD). The TMD consists of a mass-spring-damper system externally linked to the structure (**Bigdeli and Kim, 2016**). According to **Beneveli (2002)**, the goal of a TMD is to decrease the energy of the structure when it is under dynamic loads. By transferring part of the energy from the structure to the TMD, the effects of vibrations on the structural system are attenuated. In his work **Gómez (2007)** states that a TMD can reduce the impacts of vibrations on structures at certain frequencies as it is a system that dispenses with external energy sources becomes economical, requiring little maintenance and not requiring high technology. According to **Hadi and Arfiadi (1998)**, passive control systems are widely used because of their practicality in facilities and handling. On the other hand, a semi-active control system that requires an amount of external energy, although small, can be introduced into the system so that the control can be performed. The external energy introduced helps to produce a high-intensity control force, which acts by dynamically altering the structural damping coefficient. In turn, in an active vibration control system, a force is applied to the mass of the damper. The sensors and processors that exist in the operation of the system work together to evaluate the force needed to be employed in real-time, improving the performance of the damper. However, these systems require the use of a lot of energy, besides requiring more complex algorithms for their implementation, which makes them less economically attractive, says **Gómez (2007)**.

Vibration attenuation studies in buildings have considered both passive and semi-active systems. In the field of passive systems, studies conducted by **Banerji and Samanta (2011)** demonstrated the effectiveness of different configurations of a hybrid tuned liquid buffer, where a tank with water is fixed to a secondary mass, which in turn is tied – utilizing springs – to the structure that undergoes seismic action at its base. The study used a numerical model to obtain the dynamic response of a mass connected to the hybrid damper, changing the stiffness values of the springs and the ratio of the water mass with the secondary mass. Later, **Banerji and Samanta (2011)** extended **Ikeda's (2009)** studies to buildings, adding the cited equipment on each of the floors, using different mounting configurations.

Within the scope of semi-active control systems, **Gómez (2007)** states that these do not require much energy and can have their properties altered throughout the control, working in regions of different frequencies. They are, in fact, the combination of passive and active systems. Despite the relative economic advantage, there is the fact that these systems operate very frequently with batteries, therefore presenting a great risk in the case of seismic events, since the power source can be cut off. **Loh and Chao (1996)** compared tuned, passive, and active mass damper systems, passive and active base insulation systems, and active isolation systems. In the study, the acceleration and displacement of the base of the building are compared according to each isolation strategy. Currently, research has focused on variable stiffness vibration control systems, as seen in **Gupta and Pradyumna (2022)**, **Li et al. (2022)** and **Sharma et al. (2022)**. In this field of study, **Moutinho (2007)** developed a vibration control system based on the alteration of stiffness in a building using variable stiffness devices. In this case, diagonal devices were installed on specific floors of the building, which consisted of hydraulic cylinders regulated by valves, which allowed to instantly control the locking or unlocking of the bars, mobilizing, or demobilizing their axial stiffness.

According to **Liu et al. (2020)**, a variable stiffness mechanism is one capable of achieving the necessary stiffness according to the external load. According to the authors, the mechanisms of variable stiffness can equally be passive or active. In the case of liabilities, the stiffness of the spring varies according to the equilibrium position and is reached according to the configuration of the external forces. In assets, stiffness can vary without dependence on an external load. However, these systems require independent energy inputs to perform active stiffness adjustment. Also, concerning variable stiffness systems, recently, **Dantas et al. (2021)** elaborated a numerical study using the concept of spring stiffness established as a function of the force imposed on the system. This study aimed to evaluate the feasibility of using variable stiffness springs in the control of dynamically requested mechanical systems. As a validation resource, computational modelling was performed through the MEF, in which a translational spring was connected to the end of a simply supported beam (as seen in **Linn, 2004**) according to its longitudinal direction. The beam was axially compressed by a normal force of different intensities. The axial force was judged mathematically capable of modifying the stiffness of the beam. The results, however, showed a good response of the variable stiffness springs in the solution of the problem, so that the natural frequency of the beam was not modified, which allowed the initial operating conditions of the system to be kept the same.

3. Computational Simulation

The computational modelling performed in this work was based on FEM and elaborated through the program **SAP2000 (2017)**. It is a structure set of an idealized six-story building, including the ground floor and roof. In the model, columns and beams were represented by unidimensional elements under Bernoulli-Euler theory (**Bauchau and Craig, 2009)**, and floors were associated to bidimensional elements under shell theory (**Ventsel et al., 2002**). The constructive aspects were established according to **ABNT NBR 15421 (2006)**, of the Brazilian Association of Technical Standards (ABNT), which

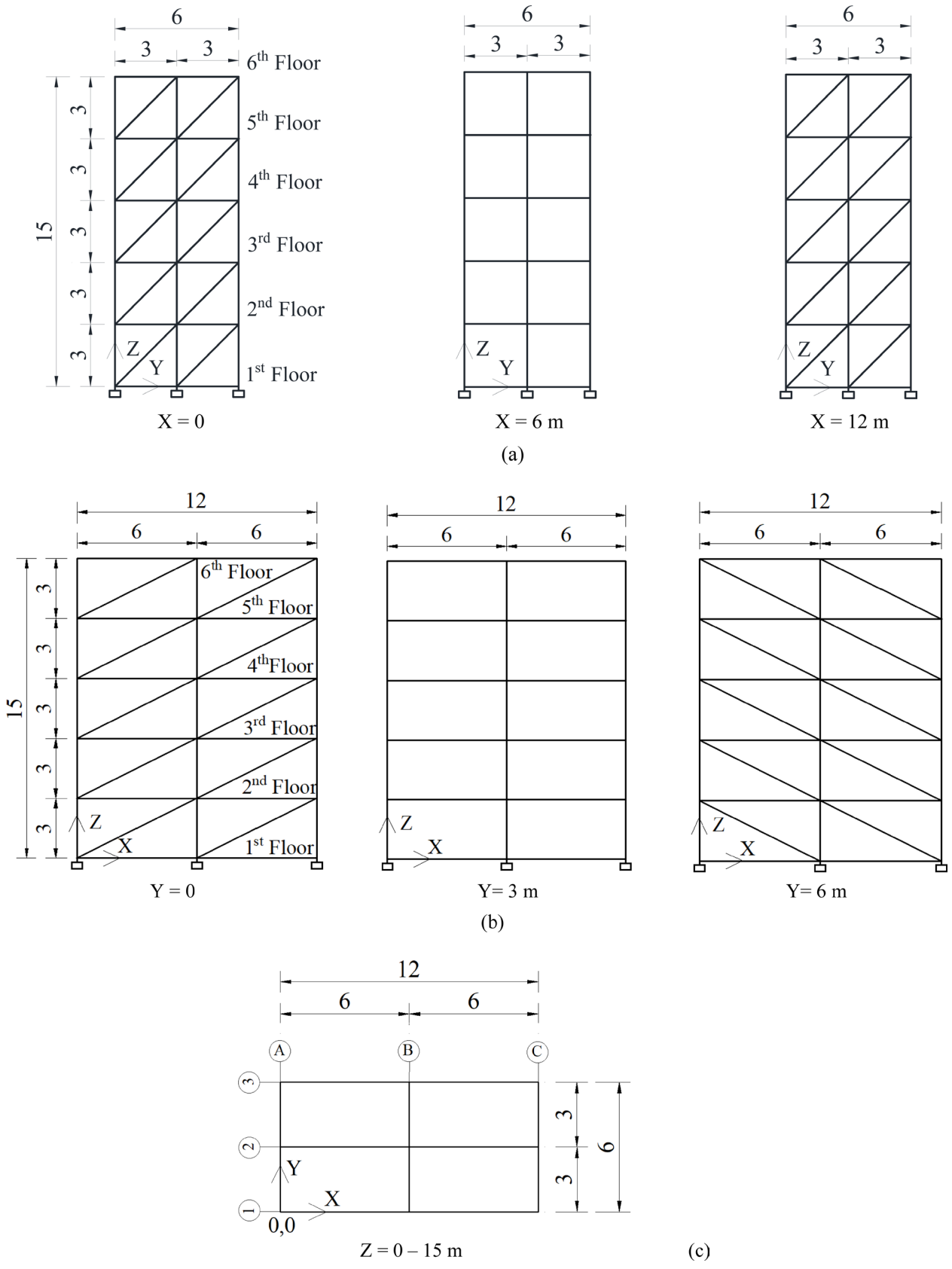

Figure 1: Building's dimensions (in meter "m" where not indicated): (a) YZ plane, (b) XZ plane, (c) XY plane.

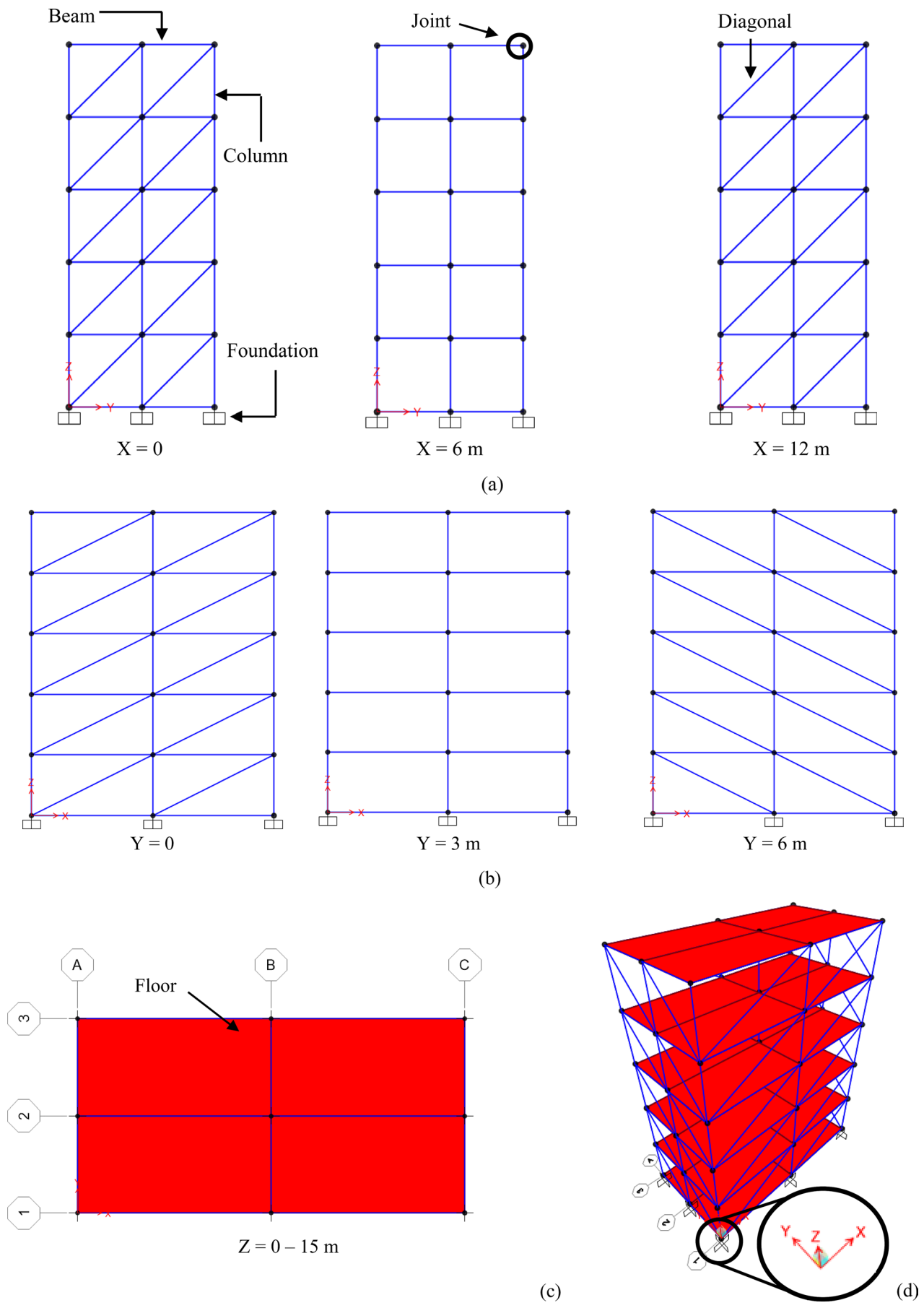

Figure 2: Computational model via FEM: (a) YZ Plane, (b) XZ Plane, (c) XY Plane, (d) Isometric view and origin point.

Table 1: Materials properties

Properties	Type of Material		
	Steel – ASTM A36	**Concrete – C25**	**Steel – ASTM A955M (G75)**
Density (kg/m^3)	7.849 x 10^3	2.549 x 10^3	7.849 x 10^3
Modulus of Elasticity (N/m^2)	1.999 x 10^{11}	2.000 x 10^{10}	1.999 x 10^{11}
Poisson Coefficient	0.26	0.20	0.30
Assigned Structural Element	Beams	Columns	Rebar

ASTM = American Society for Testing and Materials; C = Category; G = Grade; N = Newton; m = meter; kg = kilogram.

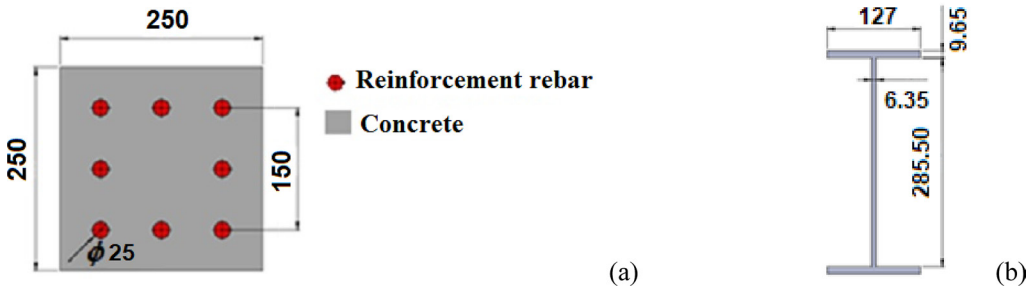

Figure 3: Sections: (a) reinforced concrete columns, (b) steel beams and diagonals (all dimensions in millimetres)

guides the design of structures subject to earthquakes, including modelling criteria. The building's dimensions are shown in **Figure 1.** By adopting an X, Y, Z Cartesian coordinate system, the building has YZ and XZ as its vertical planes, and XY as the horizontal plane. The YZ plane has 0 (A), 6 m (B), and 12 m (C) as abscissas on the X axis; the XZ plane has 0 (1), 3 m (2), and 6 m (3) as ordinates on the Y axis and the XY plane has 0, 3 m, 6 m, 9 m, 12 m, and 15 m as heights in the Z direction. The construction presents relations between its dimensions as follows: horizontally 2 times; vertically (aspect ratio) 2.5 and 1.25 times. So, horizontally the building is characterized as having one well-defined transversal dimension (Y) and another longitudinal (X). The numerical model is schematically represented in **Figure 2**, The structure was fixed at the base at the foundation level, and it is mainly formed by the association of vertical planar frames and horizontal floors. To the planar frames, diagonal-shaped locking was assigned to externally situated planes, connecting adjacent floors. These diagonals have been used in building structures with the objective of bracing the system against horizontal actions, adjusting the structural stiffness for controlling vibrations and/or reducing lateral displacements that might occur (**Palermo et al., 2015**; **Hwang et al., 2007; Sabelli, et al., 2003**).

The materials used in the various elements are listed in **Table 1**, as well as their mechanical properties. The dimensions of the cross-sections of beams and columns are illustrated in **Figure 3**. Shell elements were admitted as having a thickness of 0.1 meters and made of reinforced concrete. Reinforced concrete is a composite material that essentially consists of an association of concrete (aggregates and hydraulic cement), and structural steel called reinforcement. The basic design hypothesis assumes a perfect adhesion between these materials after hardening the concrete (**Magalhães et al., 2022)**. Although the creep effect due to the rheological behaviour of the material exists for the hardened concrete as indicated by **Magalhães et al. (2023**) this is not being considered in analysis. The material's density was included in the computational analysis because it represents an important aspect for the spatial mass distribution of the system (**Wahrhaftig et al., 2021**). Similarly, the material's Poisson coefficient and the modulus of elasticity are fundamental factors on structural vibrations analysis (**Xu and Deng, 2016**; **Laura et al., 1996**; **Duffin, 1969; Pradhan et al., 1969**).

In the first stage of analysis, the frequencies of the two first natural modes of vibration of the structural system (Modal Analysis) were obtained. In Modal Analysis, it is of interest to record that the solution is algebraically obtained by eigenvalues and eigenvectors from Eq. (1), results in Hertz, which is based on the characteristic equation composed of the generalized mass (M) and stiffness (K) matrices of the system, The values for the respective natural vibration frequencies and modes of the analysed structure are shown in **Figure 4**.

$$f = \frac{1}{2\pi}\sqrt{\frac{K}{M}} \quad (1)$$

In the second analysis stage, the time-dependent displacements of nodes of the structure were observed under the action of seismic accelerations before the application of the springs of variable stiffness aiming to define the most unfavourable point, or points, of the system

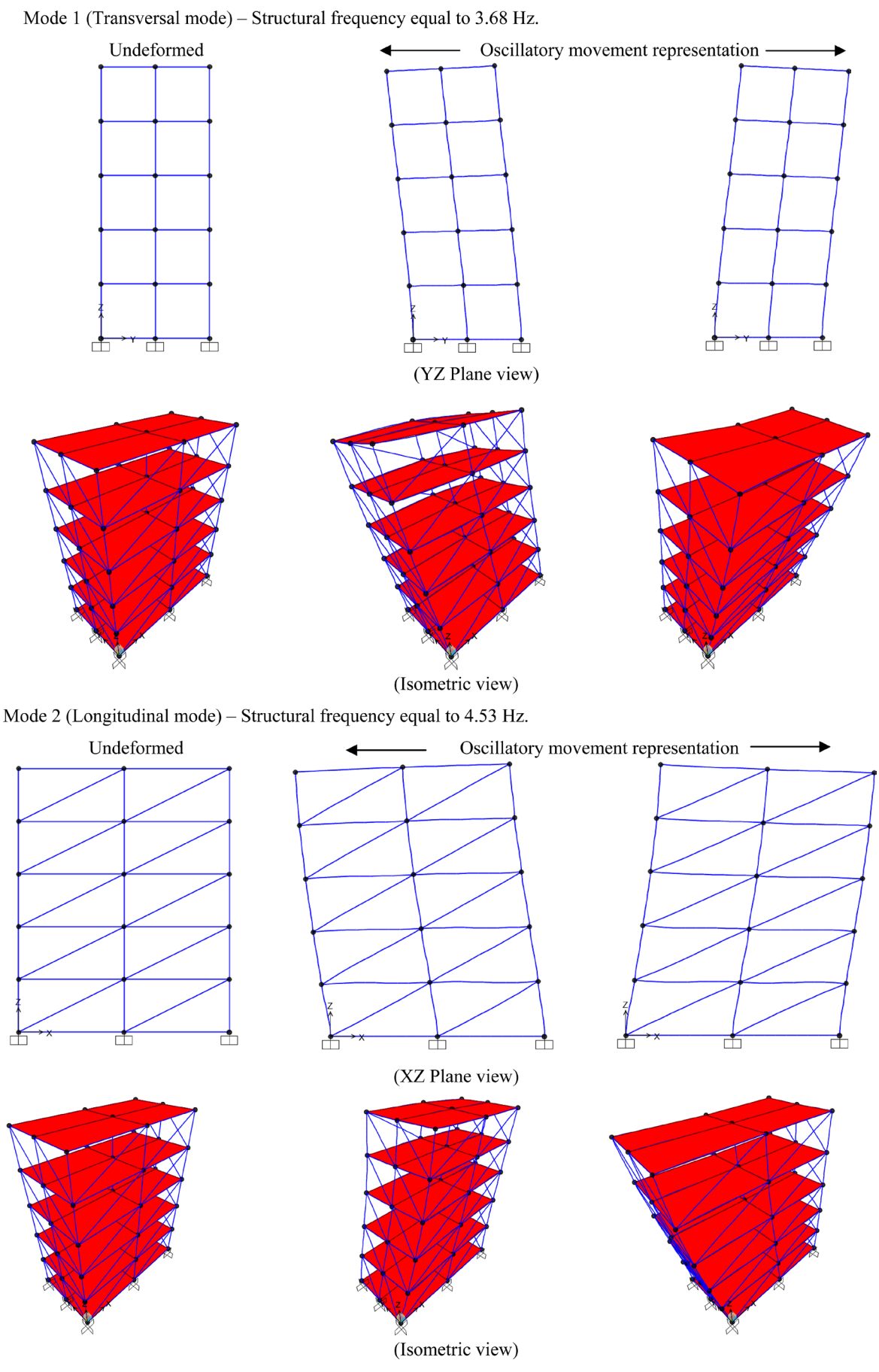

Figure 4: Natural vibration frequencies and modes

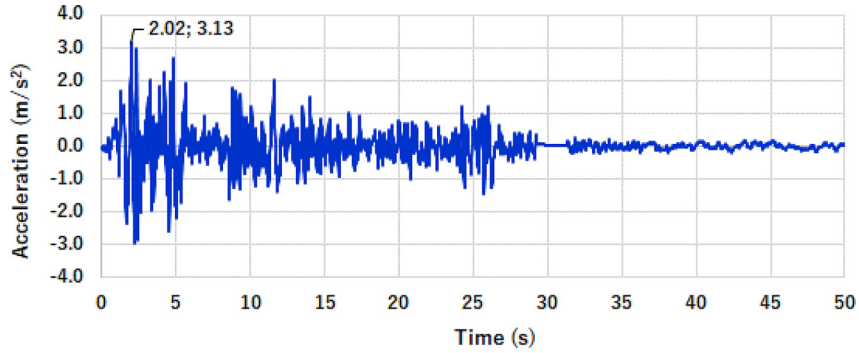

Figure 5: Time history acceleration of "El Centro" earthquake - north-south component

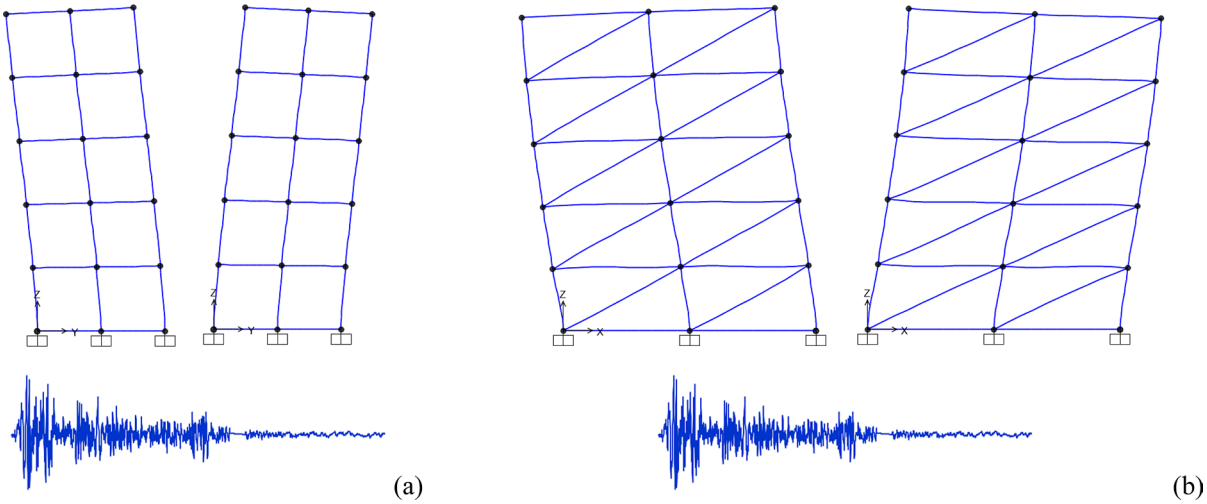

Figure 6: Representation of the unidirectional seismic activity on the building: (a) YZ plane – earthquake acting in the Y direction), (b) XZ plane – earthquake acting in the X direction).

in terms of displacement and the corresponding time step. These accelerations are related to the particularly seismic action of the event designated as "El Centro" and were imposed on the base of the structure. It is important to mention that this seismic event occurred in the city of El Centro, California, United States of America, and was recorded as having a magnitude of 6.9 on the Richter scale (maximum 9). The peak acceleration captured by seismographs to the north-south component was 3.13 m/s², approximately 0.32 g, which occurred 2.02 seconds after the event to have been registered. The accelerations in time domain for the aforementioned earthquake component can be seen in **Figure 5** (**vibration data, 2022**; **Zhan et al., 2022**; **Singh et al., 2020**).

In the mathematical-numerical-computational model, the accelerations described in **Figure 5** were inserted as a time-history function given the nature of their variation. The solution to the problem, in this case, occurs by solving the dynamic equilibrium equation, Eq. (2), by the direct integration method,

$$K\,u(t)+C\frac{d}{dt}u(t)+M\frac{d^2}{dt}u(t)=r(t) \qquad (2)$$

where K, C and M are the matrices of stiffness, damping and mass, respectively, and u and r are the displacement and resulting force vectors, both time quantities. The representation of the derivative, first and second, obeys Leibniz's notation.

The third stage of the analysis begins after the application of the time series associated with the seismic accelerations of the mentioned event to the structural system, alternatively to Y and X directions, each one in turn, as schematically represented in **Figure 6**. Acceleration loads were determined by d'Alembert's principle, and are associated with the earthquake time series. These loads are computed for each joint and element, and are simply equal to the negative of the joint translational masses in the joint local coordinate system, representing this way inertia forces (**SAP2000, 2017**). The computational processing was conducted under a linear hypothesis considering a 5% of damping applied proportionally to stiffness and mass matrices (**Zhou and Li, 2022**). The event duration was divided into 0.02 seconds time intervals, totalizing 2500 steps. The loading due to the self-weight was not considered but the masses of the structural pieces themselves were taken into account. Wind effects of any type are not computed. Similarly, instability analysis was put out of the present context either by using springs (**Tanaka et al., 2023**) or not (**Murawski, 2022** and **2021**; **Wahr-**

Table 2: Absolute displacements at the building section of maximum displacement

Y:	Time step 0.58 seconds		X:	Time step 0.66 seconds	
H (m)	**Joint**	**Displacement (mm)**	**H (m)**	**Joint**	**Displacement (mm)**
15	53	4.235274	15	46	2.491800
12	44	3.237544	12	37	2.286832
9	35	2.114802	9	28	1.944135
6	26	1.079251	6	19	1.433066
3	17	0.339519	3	10	0.768747
0	8	0	0	1	0

H = height; m = meter; mm = milimeter

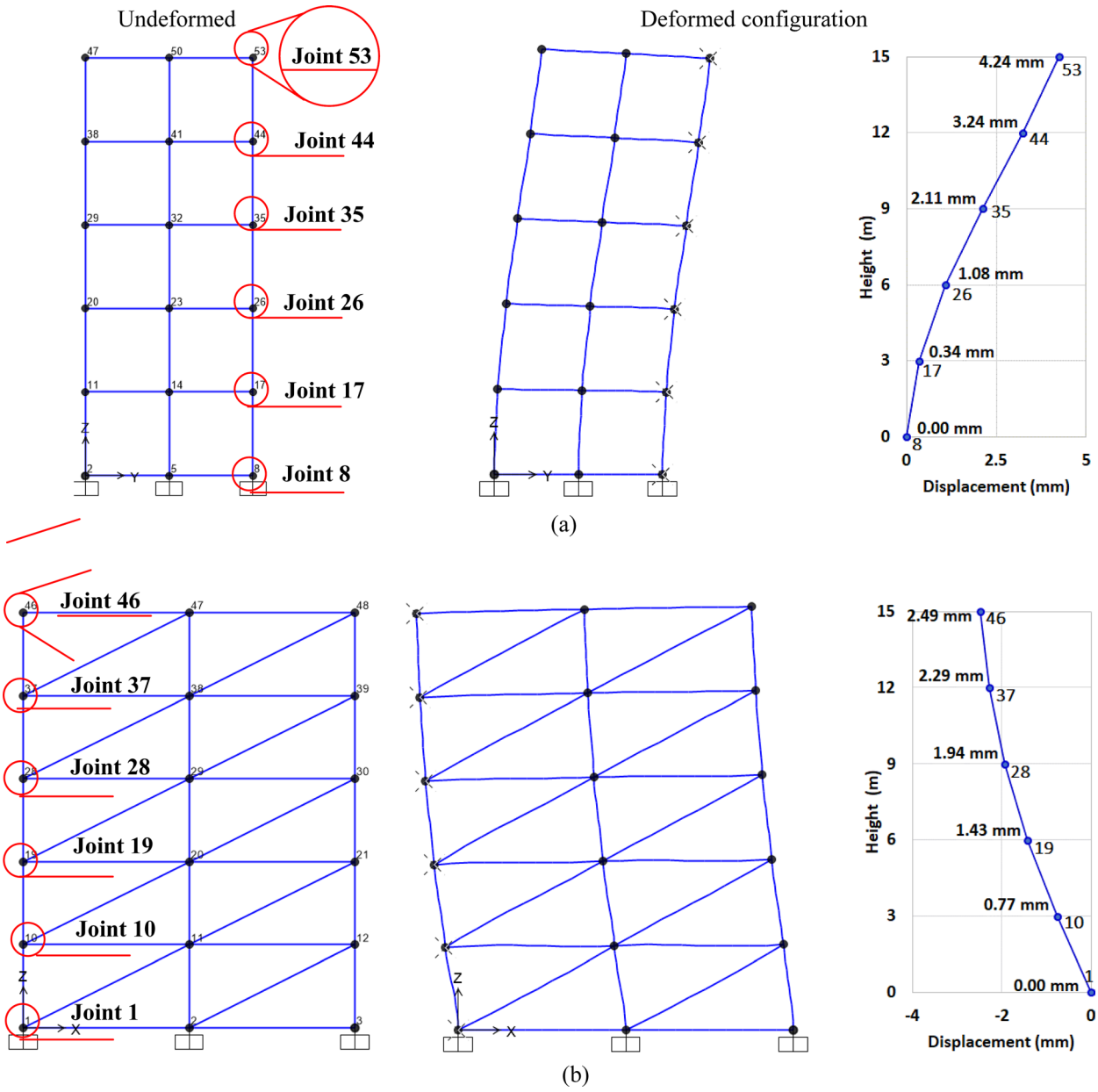

Figure 7: Building sections at the planes of maximum displacements: (a) YZ Plane – X = 6 m. Time step 0.58 seconds. Earthquake acting in the Y direction; (b) XZ Plane – Y = 0. Time step 0.66 seconds. Earthquake acting in the X direction.

haftig, 2020). Then, springs were applied according to the earthquake action to the superior connection of diagonals of planes around the building. Stiffness coefficients to these springs were studied in order to keep the strucutural frequencies as close to the initial values as possible.

4. Results and Discussion

4.1. Displacements and frequencies analysis

4.1.1. Original system

The numerical simulation was performed as described in the third stage of the analysis by initially examining the structure before the application of springs, named as the "Original System". With this, it was possible to select the most unfavourable joint in terms of displacement, i.e. the extreme relative value presented by a joint, or joints, considering the earthquake independently acting in both horizontal directions, transversal (Y) and longitudinal (X). **Table 2** summarizes the obtained results for the previously mentioned directions.

Figure 7 shows the undeformed and deformed configurations of the building sections that contain the joints of maximum displacements, which are highlighted by a

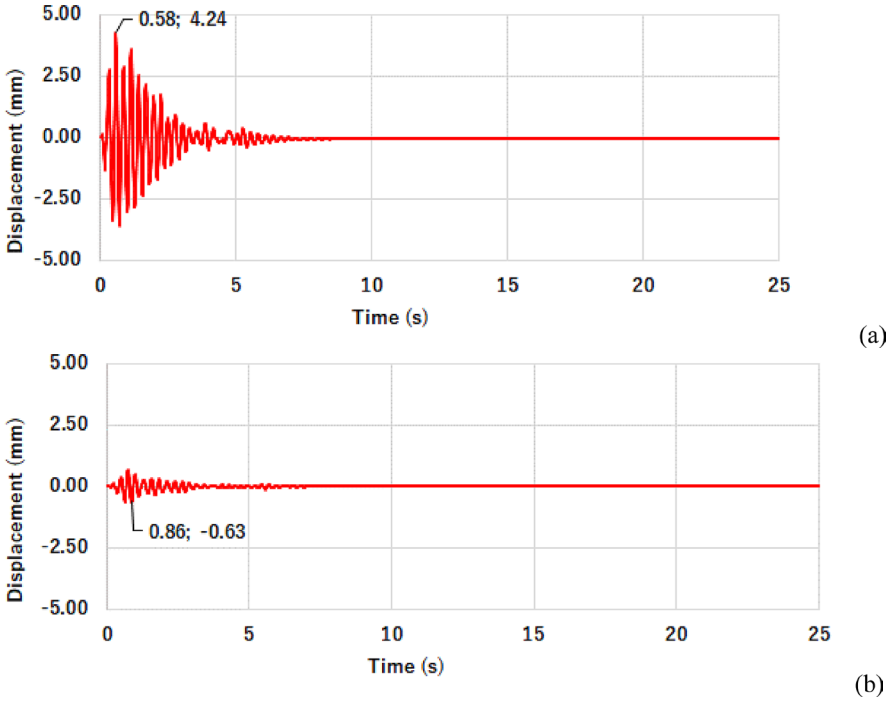

Figure 8: Time series of the joint 53 under earthquake acting in the Y direction. Response to (a) Y and (b) X directions

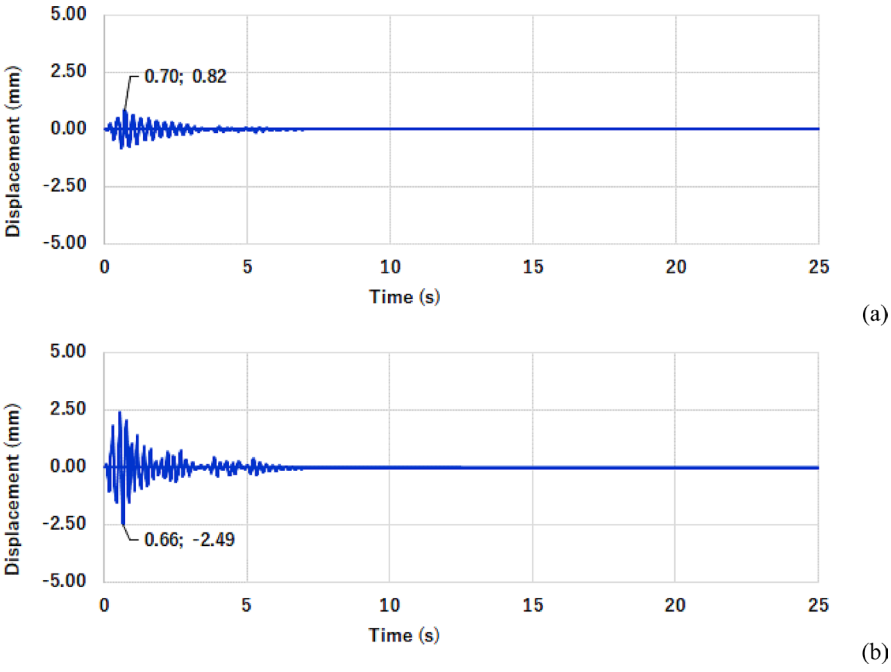

Figure 9: Time series of the joint 46 under earthquake acting in the X direction. Response to (a) Y and (b) X direction

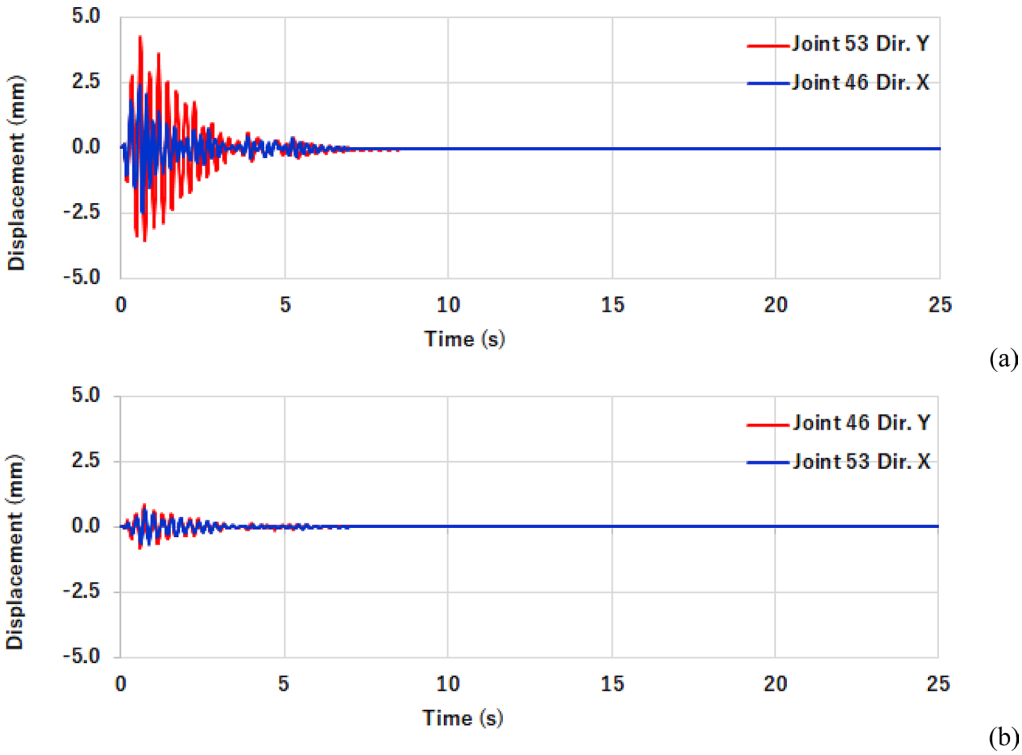

Figure 10: Compared time series of the reference joints regarding the (a) primary and (b) secondary movements

circle, at the corresponding time step. The deformed configuration given by the group of displacements along the building height at these sections can be correlated to the first and second modes of vibration, respectively, as indicated in **Figure 4**. The angle obtained relating the maximum displacement with the building height is 0.016 degrees for the Y direction, and 0.010 degrees, for the X direction.

As can be seen in **Table 2**, the joints of number 53 and 46 presented the extreme displacements respectively for the Y and X directions. For that reason, they were chosen as the reference point for the evaluation of the group of springs to be inserted (control system). Therefore, the evaluation of the structural response after the application of springs was based on the Fast Fourier Transform (FFT) performed on the time series of displacements presented by the reference points. As identified in the analysis, the maximum displacement of 4.24 mm occurs 0.58 seconds after the seismic event reaches the building, regarding the Y direction, and of 2.49 mm occurring 0.66 seconds relatively to the X direction. These displacements are related to the "primary" structural movement, that one that is oriented according to the same direction as the seismic action. The other one, which occurs orthogonally to that is named as the "secondary" movement. The complete time series of displacements of the selected joints for the building transversal (Y) and longitudinal (X) directions, for both primary and secondary movements, can be observed in **Figure 8** and **Figure 9**. So, it is possible to see that the secondary movement of the structure is 16% and 33% of the primary ones. The time steps in which the largest displacements occur are all different from each other, and from the time step of the peak earthquake acceleration (see **Figure 5**). For the two conditions of earthquake activity, the vertical displacements (Z) are not too representative. The peaks in the Z direction to the passage of the earthquakes respectively represent 10% and 11% of the maximum obtained values.

For comparative purposes, the displacements of both reference joints with respect to the primary and secondary movements can be seen in **Figure 10**, letters (a) and (b), respectively.

4.1.2.Modified system

It is important to have clear that the idealized control system is composed of translational springs associated with the connecting elements between floors, or diagonals, applied to peripheral YZ and XZ planar frames of the building. The structure so formed is designed as the "Modified system". Different values of stiffness, or spring coefficient, were assigned to the mentioned springs through the partial release option, as indicated in **Figure 11**, seeking to keep the working conditions of the structure as close as possible to the initial design parameters during the earthquake action. The effect of using the partial release option is similar to applying a spring to the chosen extremity of an element because this allows the assigned extremity to work as a spring with the stiffness coefficient value which was defined for it.

It is important to remember that in the present study, springs were applied to the diagonals contained in the

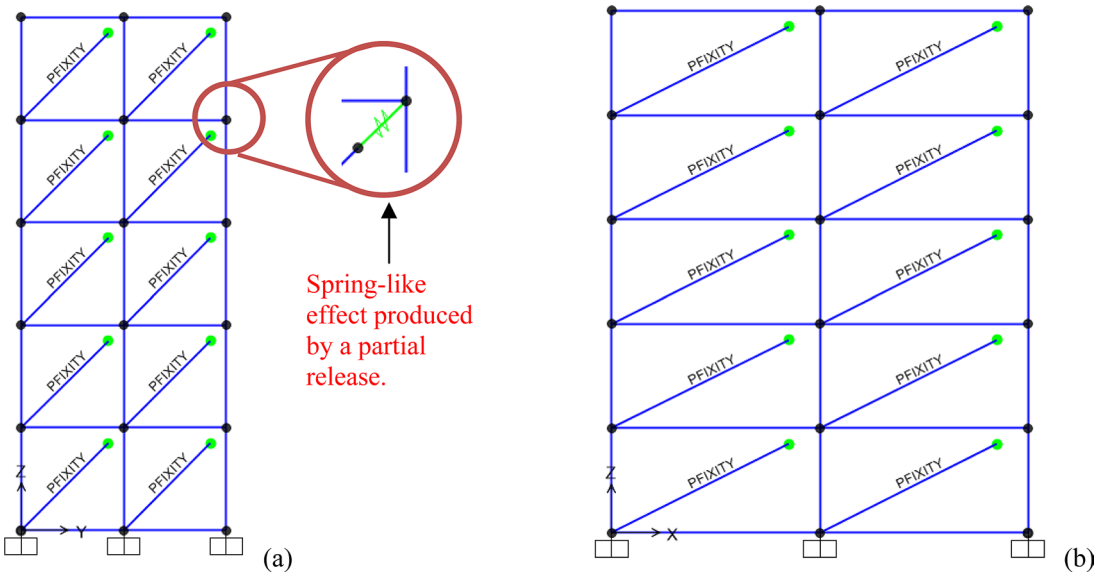

Figure 11: Building model with the application of springs in building peripheral planes (a) YZ, and (b) XZ

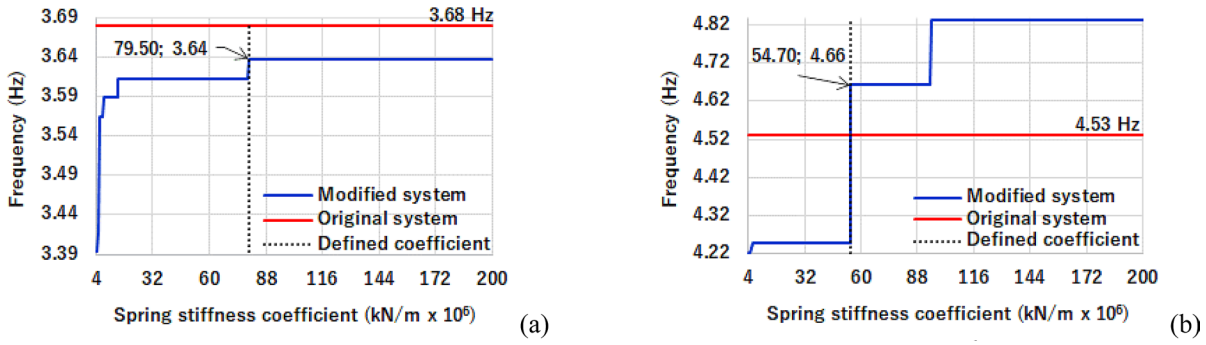

Figure 12: Path taken to define the spring coefficients: (a) 1st mode (Y direction) and (b) 2nd mode (X direction).

Table 3: Structural frequencies (in Hz) for Modal Analysis and FFT.

Earthquake acting in the Y direction. Mostly associated with the first mode of vibration – Primary movement.									
Spring stiffness (kN/m)	**After springs**		**Original**		**Differences between columns (%)**				
7950000 Applied to diagonals in peripherical YZ planes	(1) Modal Analysis	(2) FFT on joint	(3) Modal Analysis	(4) FFT on joint	1-2	1-3	**2-3**	2-4	3-4
1st mode (Transversal)	3.67	**3.64**	**3.68**	3.64	-0.82	0.27	1.09	0.00	-1.10
2nd mode (Longitudinal)	4.54	3.64	4.53	3.64	-24.73	-0.22	19.65	0.00	-24.45
Earthquake acting in the X direction. Mostly associated with the second mode of vibration – Primary movement.									
Spring stiffness (kN/m)	After springs		Original		Differences between columns (%)				
5470000 Applied to diagonals in peripherical XZ Planes	(1) Modal Analysis	(2) FFT on joint	(3) Modal Analysis	(4) FFT on joint	1-2	1-3	**2-3**	2-4	3-4
1st mode (Transversal)	3.68	3.64	3.68	3.64	-1.10	0.00	1.09	0.00	-1.10
2nd mode (Longitudinal)	4.51	**4.66**	**4.53**	4.66	3.22	0.44	-2.87	0.00	2.79

Obs.: Main parameters of analysis in bold character.

YZ and XZ planes, each one in turn, according to the earthquake acted in the Y and X directions, separately, not both at the same time. The building's central plans were absent of diagonals. The possibility of achieving the desired condition was proven by **Wahrhaftig et al. (2022)** through tests in a physical laboratory using a device on a natural scale, a beam made of structural steel, on which a hydraulic jack actuated according to the lon-

Table 4: Absolute displacements in the building section after applying the springs

Y:	Time step 0.58 seconds			X:	Time step 0.66 seconds		
H (m)	**Joint**	**Displacement (mm)**	**Δ (%)**	**H (m)**	**Joint**	**Displacement (mm)**	**Δ (%)**
15	53	4.234918	-0.01	15	46	2.491800	-2.56
12	44	3.246860	0.29	12	37	2.286832	-2.72
9	35	2.132708	0.84	9	28	1.944135	-2.91
6	26	1.099940	1.88	6	19	1.433066	-3.05
3	17	0.353065	3.84	3	10	0.768747	-3.09
0	8	0	0	0	1	0	0

Δ = Variation between the current value to the previously obtained (**Table 2**); H = height; m = meter; mm = millimetre

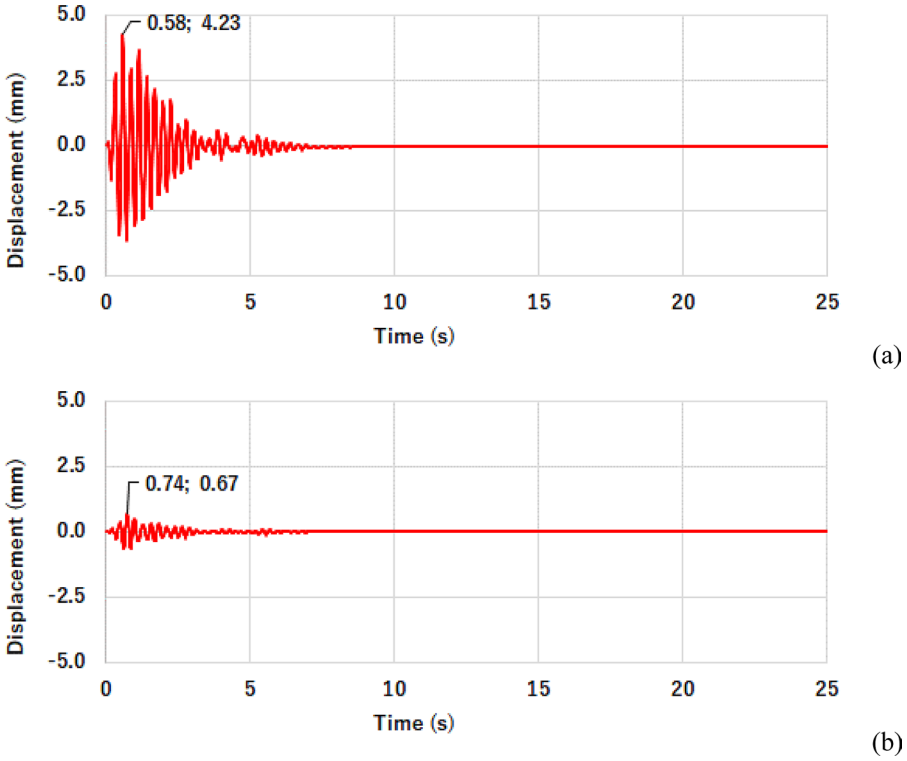

Figure 13: Time series of the joint 53. Earthquake acting in the Y direction. Modified system. Structural response to the (a) Y and (b) X directions.

gitudinal direction of it, i.e. the axis of the structural element, to take action as a control device. Mechanisms such as this were evaluated numerically by **Mahato et al. (2019)** as being an efficient control tool to mitigate displacements of buildings under seismic action.

Different values of stiffness were applied to the springs to form a control system. The path taken to define the spring coefficients is represented in the graphs of **Figure 12**. There, it is possible to see "jumps" of frequency that can reveal a nonlinear effect regarding the vibration problem, such as a base excitation (**Silva et al., 2021**). The response of the reference nodes, measured in the frequency domain, for each defined stiffness value is shown in **Table 3.** The frequencies were calculated for both original and modified systems through the Modal Analysis, Eq. (1), and FFT, Eq. (2).

By adopting a spring stiffness equal to 7950000 kN/m, applied to diagonals contained in the building's peripherical YZ planes, seismic action in the Y direction, the response of the structure calculated on the reference joint displacement is 1.09% different from the frequency of the first original natural vibration mode. When springs of stiffness coefficient equal to 5470000 kN/m are applied to diagonals contained in the building's peripherical XZ planes, the response of the reference node, in the frequency domain, occurs for the frequency of 4.66 Hz. This value is 2.87% above of the natural frequency of the second mode of vibration when calculated by Modal Analysis. Bigger values than these when adopted do not favour any change in the structural response in terms of frequency for the Y direction but do it for the X direction (see **Figure 12**). On the other hand, smaller values take

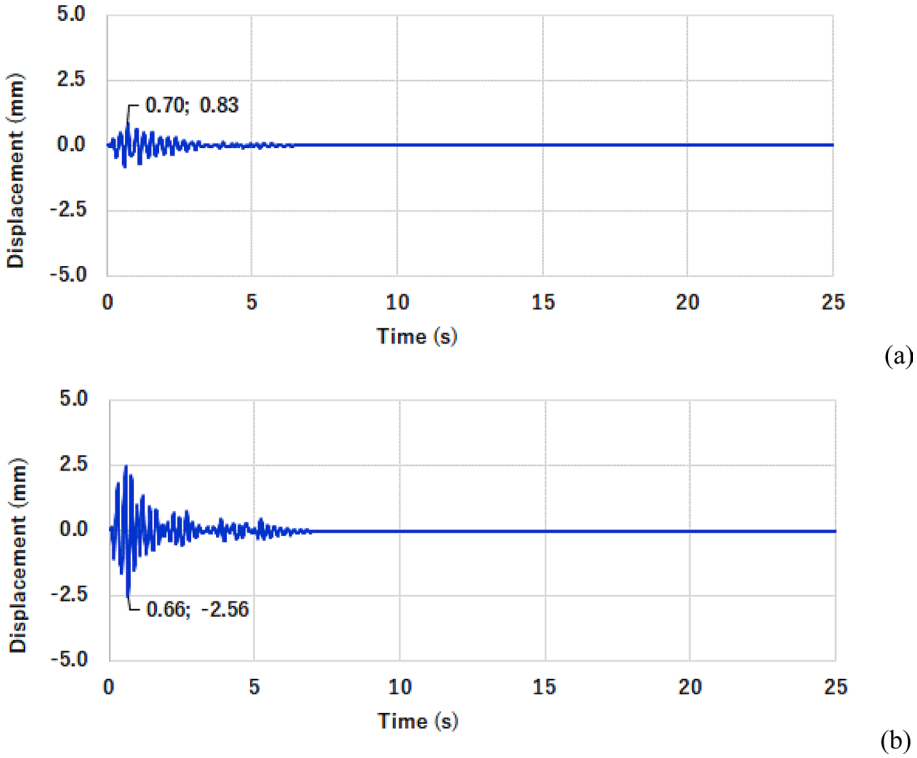

Figure 14: Time series of displacements of the joint 46. Earthquake acting in the X direction. Modified system. Structural response to the (a) Y and (b) X directions.

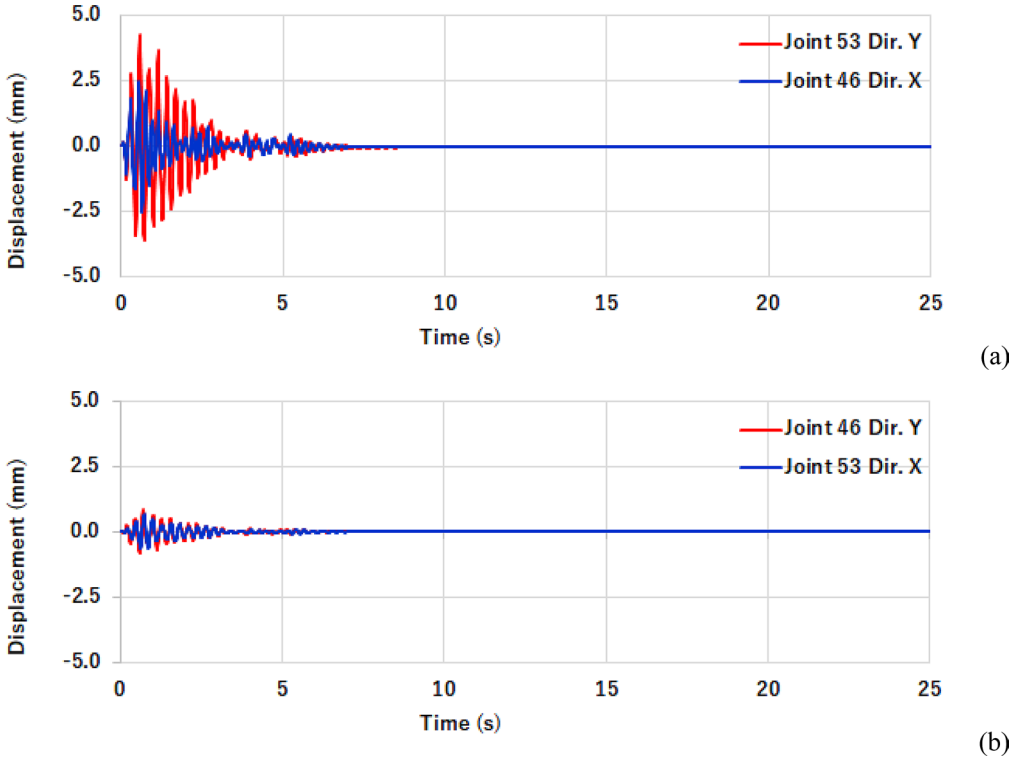

Figure 15: Time series of the reference joints regarding the (a) primary and (b) secondary movements

the structural frequencies down, and increase differences in relation to the original ones. However, larger coefficients reduce the nodal displacements in comparison with lower values. The indicated spring coefficients in **Table 3** represent 39.8 and 43.2 times the axial stiffness of the respective diagonal given by the expression K = EA/L, where E is the young modulus of the material (199000 N/mm^2), A is the cross-section area (4264.03

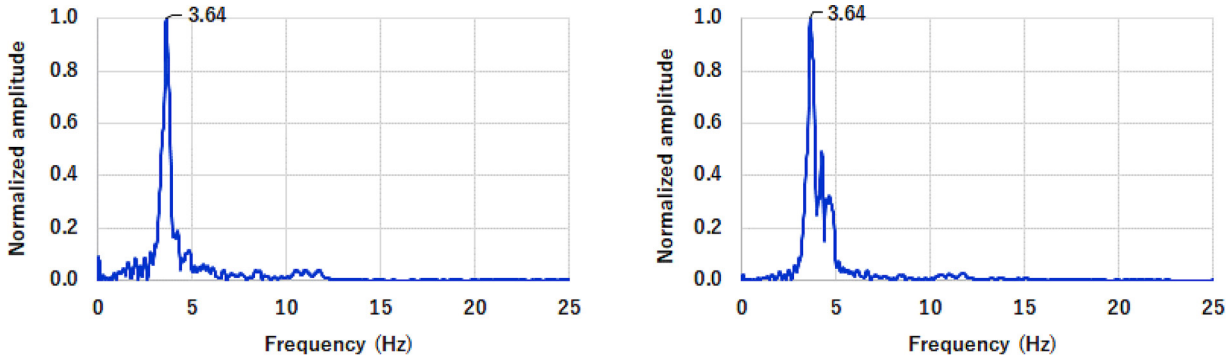

Figure 16: Frequency domain of the joint 53 under earthquake acting in the Y direction. Original system. Structural response to the (a) Y and (b) X directions.

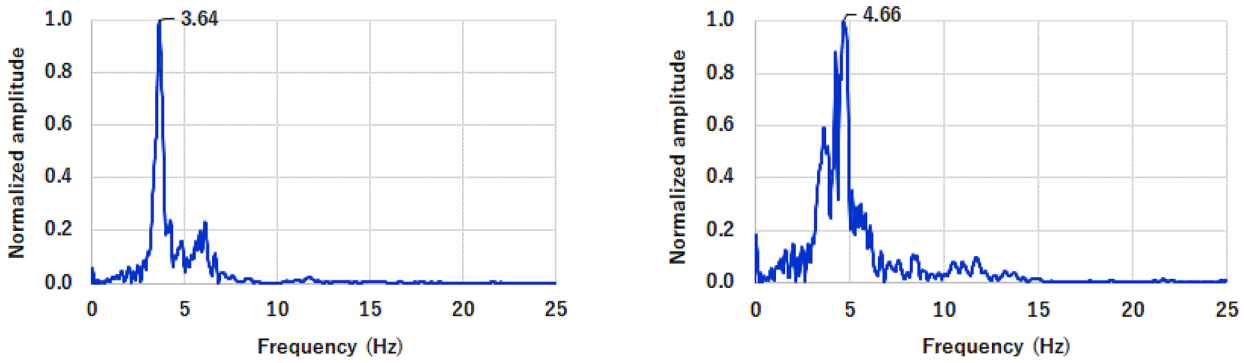

Figure 17: Frequency domain of the joint 46 under earthquake acting in the X direction. Original system. Structural response to the (a) Y and (b) X directions.

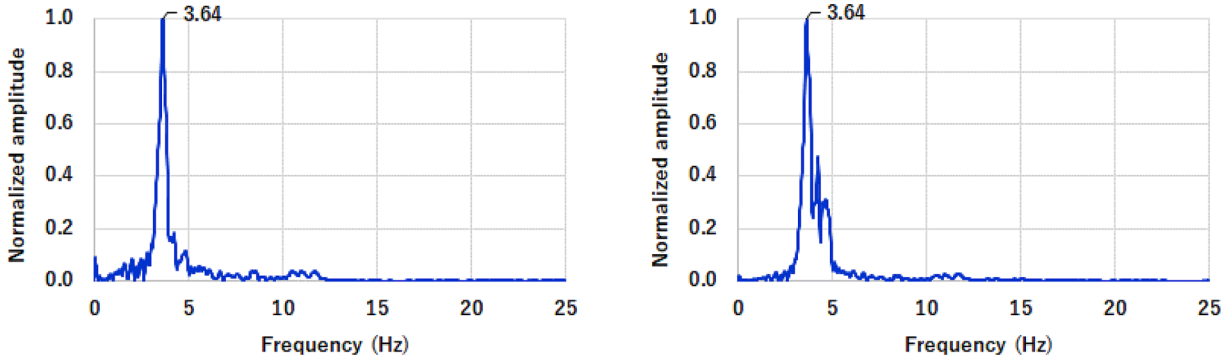

Figure 18: Frequency-domain of the joint 53. Earthquake acting in the Y direction. Modified system. Structural response to the (a) Y and (b) X directions.

mm^2), and L is the element length (4243 mm for YZ plane, and 6708 mm for XZ plane).

To the original system, there are differences of 1.10% and 2.79% when the frequency of the primary movement is computed through the Modal Analysis and FFT. This means that the earthquake mobilizes frequencies sufficiently close to the natural structure frequencies as to produce the resonance with the system. The largest difference of the Modal Analysis is 0.44% comparing results for the original and modified systems. Only when the second mode of vibration is calculated through the FFT on the secondary movements, differences around 24% are found. This aspect can be understood as the fact that the earthquake is not able of strongly mobilizing the orthogonal direction that it acts upon. Applying springs to the diagonals of peripheral YZ planes elevates the second modal frequency by 0.44%. However, this does not affect the modal frequency of the first mode consid-

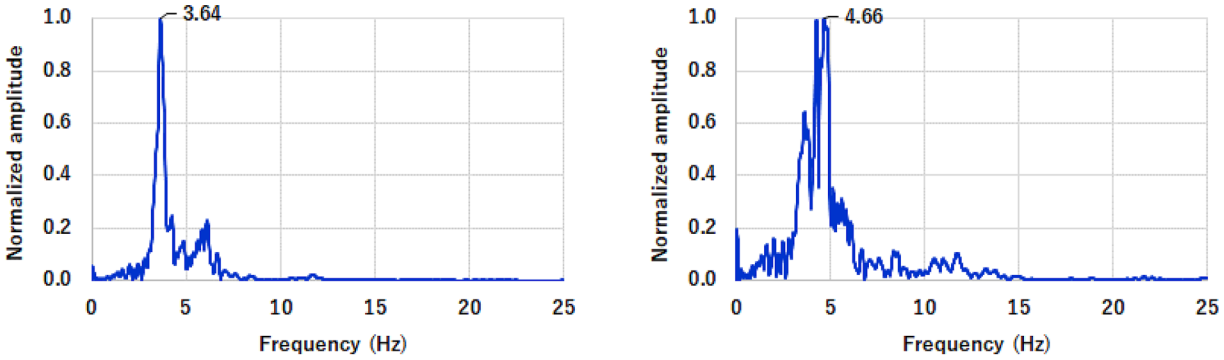

Figure 19: Frequency-domain of the joint 46. Earthquake acting in the X direction. Modified system. Structural response to the (a) Y and (b) X directions.

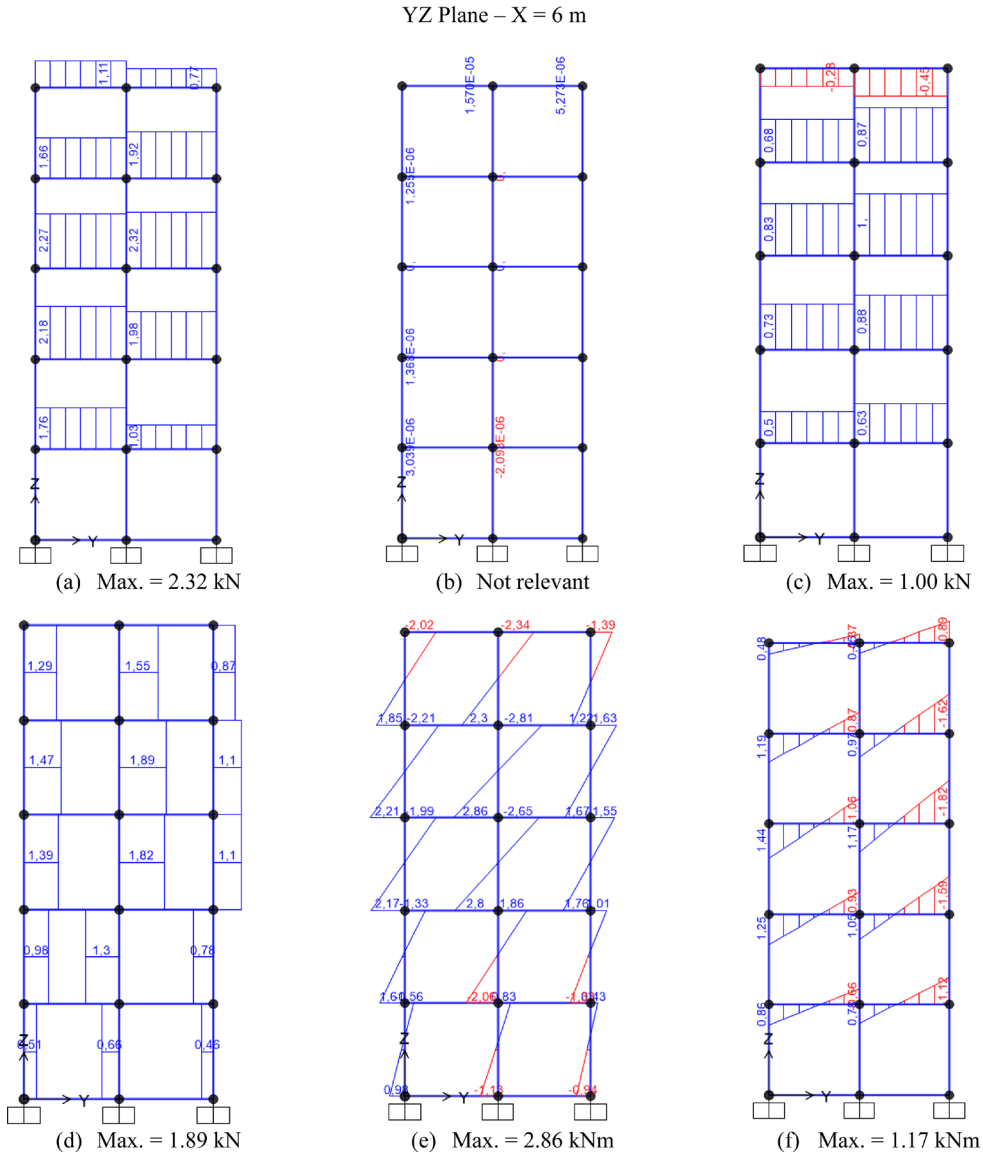

Figure 20: Forces in the building section. Original system. Time step 0.58 seconds. Earthquake in the Y direction: (a) and (g) Axial force; (b) and (h) Torsion moment; (c) and (i) Shear force in the vertical direction; (d) and (j) Shear force in the horizontal direction; (e) and (k) Bending moment flexing the vertical direction; (f) and (l) Bending moment flexing the horizontal direction.

XZ Plane – Y = 6 m

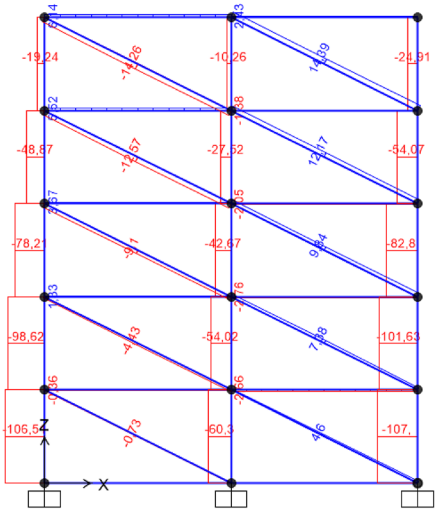

(g) Max. = 107.00 kN

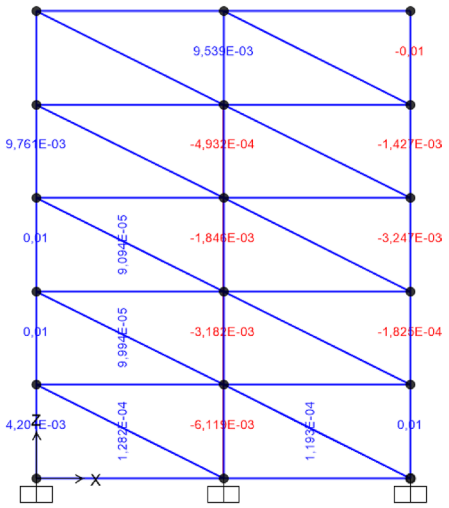

(h) Not relevant

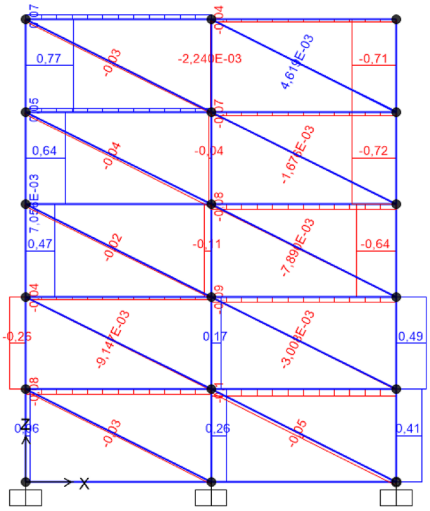

(i) Max. = 0.72 kN

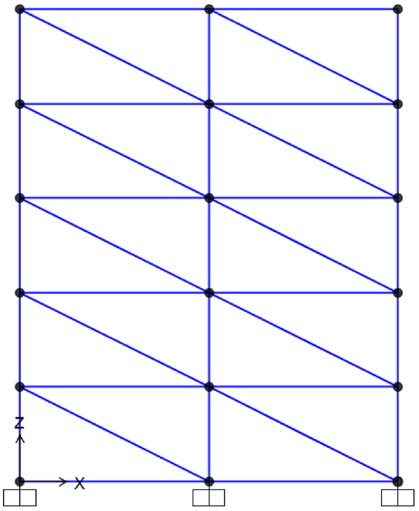

(j) Null

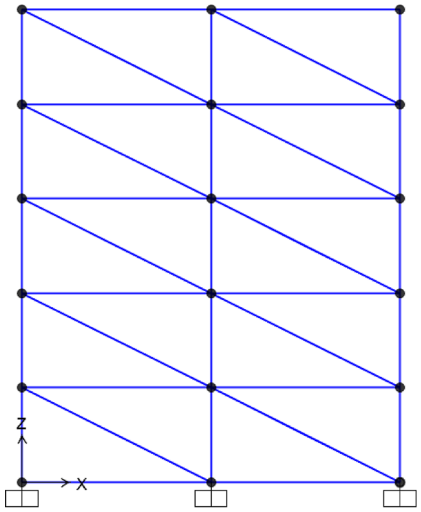

(k) Null

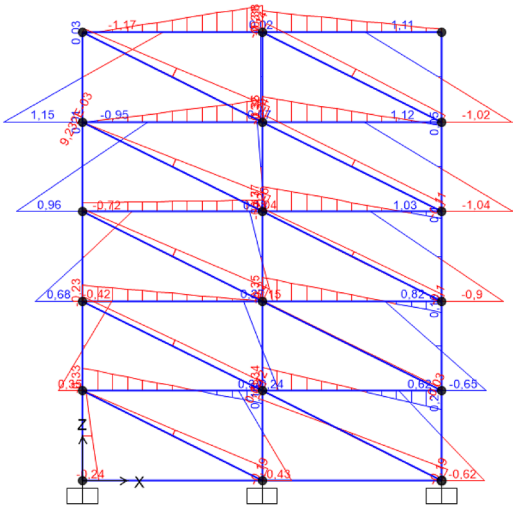

(l) Max. = 1.04 kNm

Figure 20: Continued

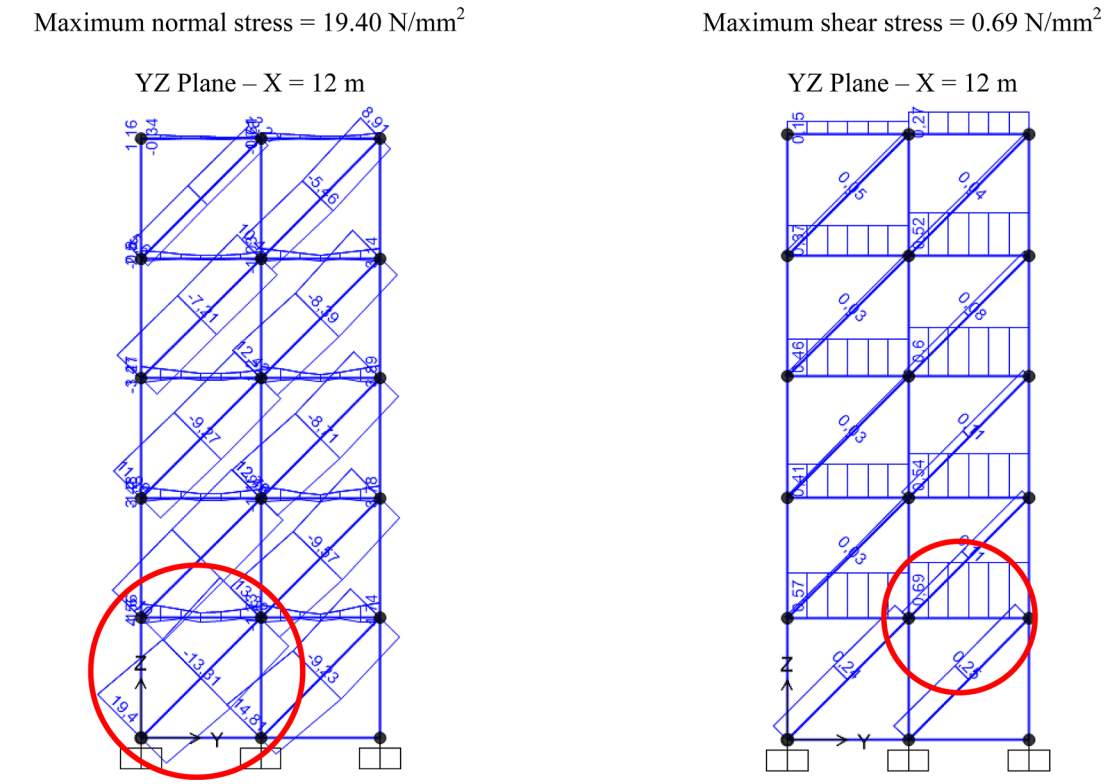

Figure 21: Envelope of maximum/minimum stresses in the original system. Earthquake in the Y direction.

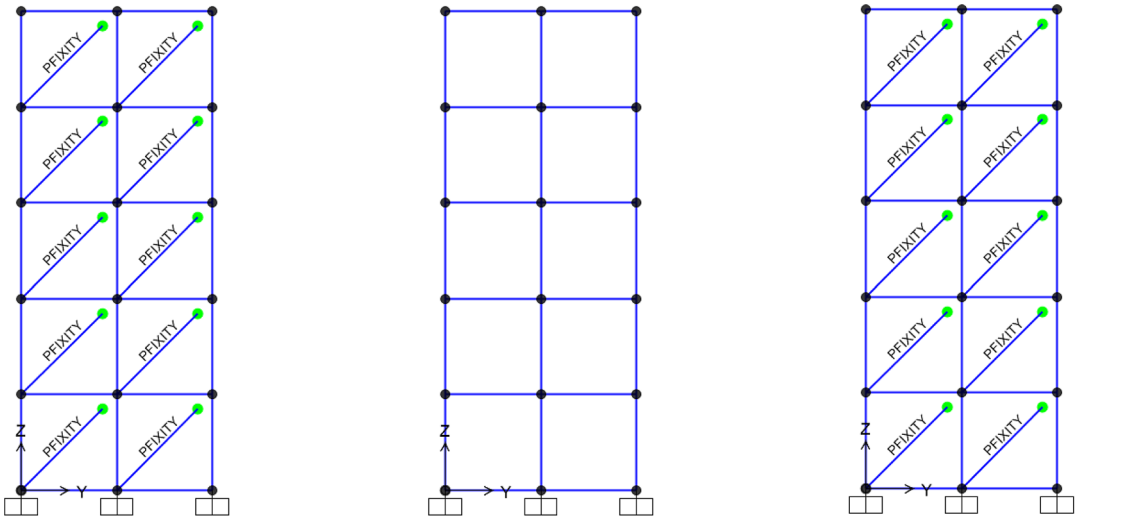

Figure 22: Modified system by applying springs to diagonal in the YZ planes

ering the same earthquake action. Assigning springs to the frame structure, the modal frequencies of the modified system are slightly reduced by 0.27% and 0.66%, 1st and 2nd modes, respectively. Therefore, the perceived relative constancy in the natural frequencies of vibration of the structure with differences of 1.09% and 2.87% indicate that, in case of a seismic shock, the dynamic characteristic of the springs could regulate the harmful effects that are transmitted to the structure and keep the vibration frequencies under a certain control.

It is important, at the same time, to consider the damped natural frequencies of the structure as references, calculated by the expression $f_d = f_n$, where f_n is the undamped natural frequency and is the damping ratio. So, the two damped natural frequencies of the structure are 3.675 Hz and 4.524 Hz, which are close to the undamped natural frequencies because civil structures are usually weakly damped (5% of damping ratio adopted). Frequencies of the original system calculated by FFT under seismic effects are 1% and 3% distant from these last ones.

YZ Plane – X = 6 m

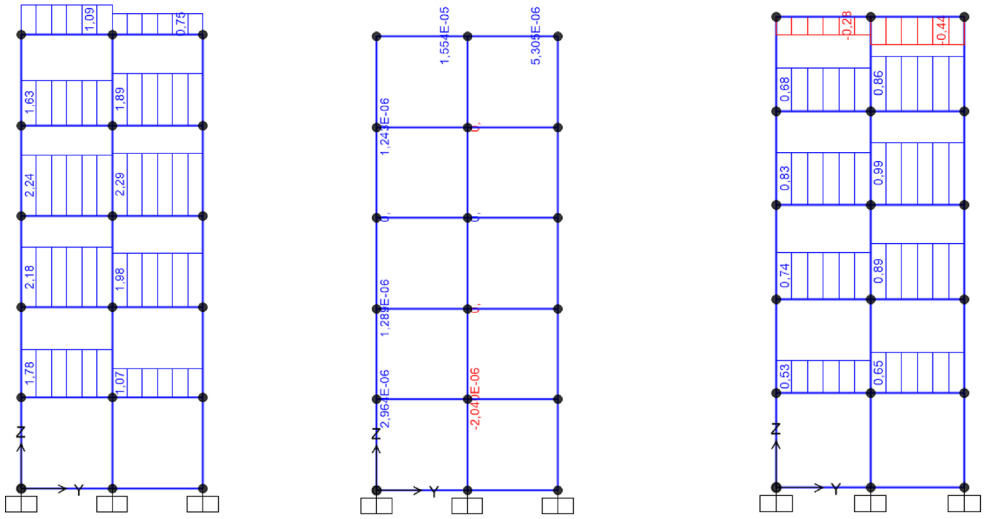

(a) Max. = 2.29 kN (b) Not relevant (c) Max. = 0.99 kN

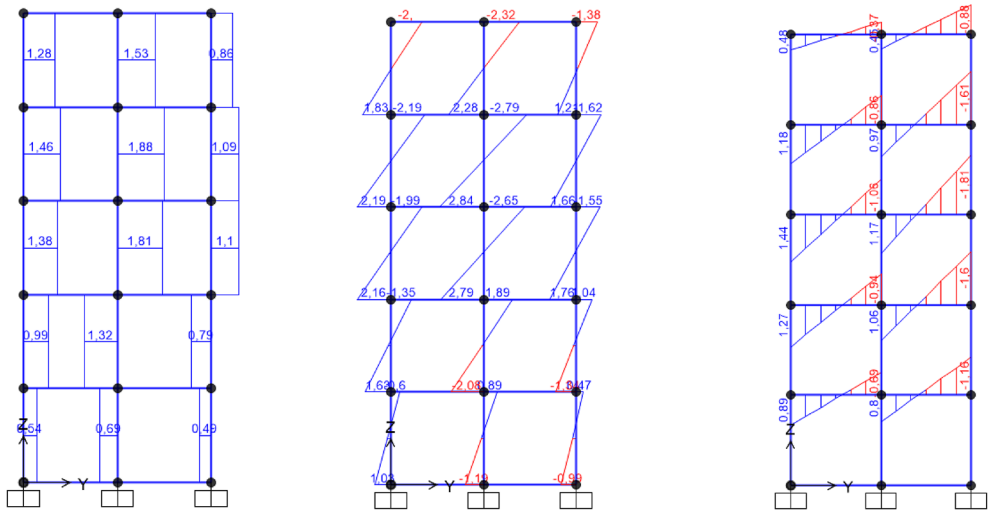

(d) Max. = 1.88 kN (e) Max. = 2.84 kNm (f) Max. = 1.81 kNm

XZ Plane – Y = 6 m

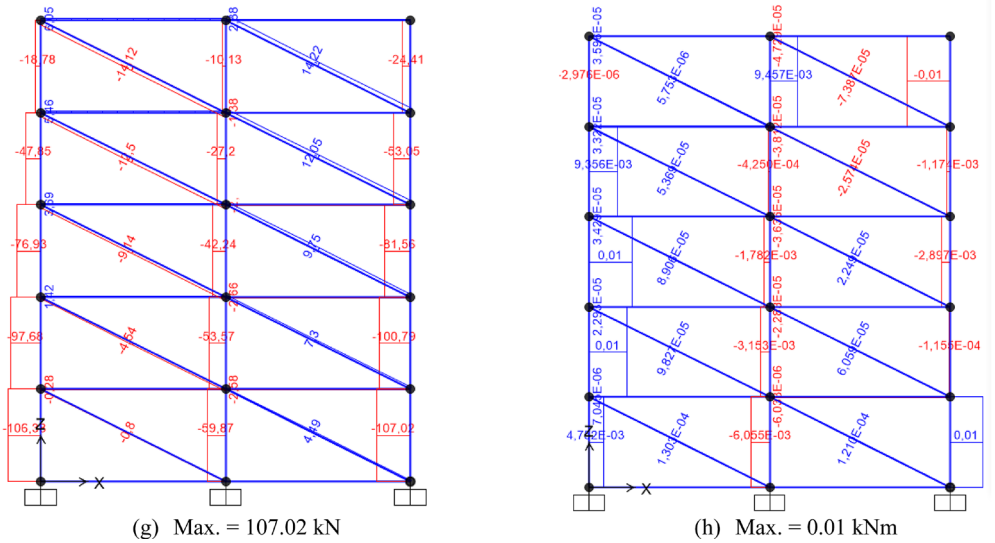

(g) Max. = 107.02 kN (h) Max. = 0.01 kNm

Figure 23: Forces in the building section of the modified system. Time step 0.58 seconds. Earthquake in the Y direction: (a) and (g) Axial force; (b) and (h) Torsion moment; (c) and (i) Shear force in the vertical direction; (d) and (j) Shear force in the horizontal direction; (e) and (k) Bending moment flexing the vertical direction; (f) and (l) Bending moment flexing the horizontal direction.

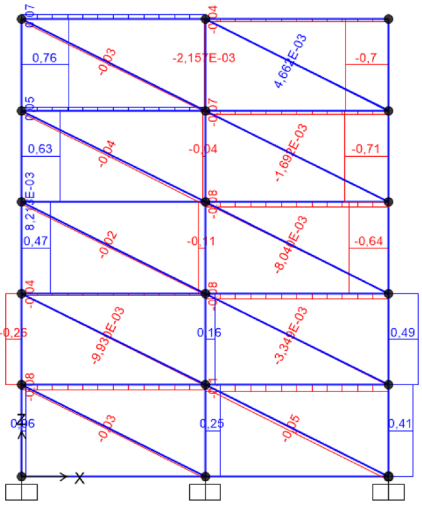

(i) Max. = 0.71 kN

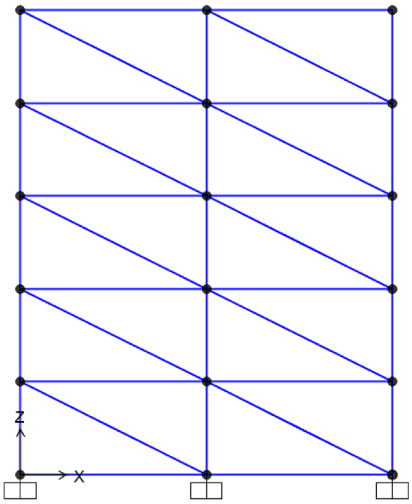

(j) Null

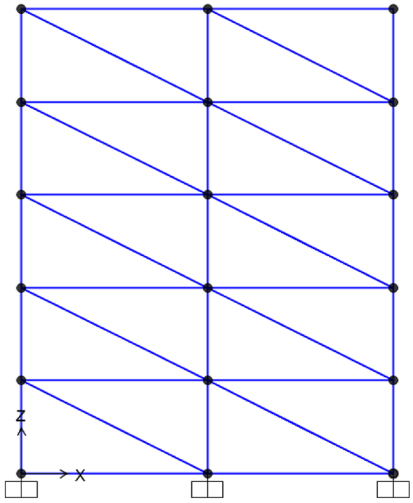

(k) Null

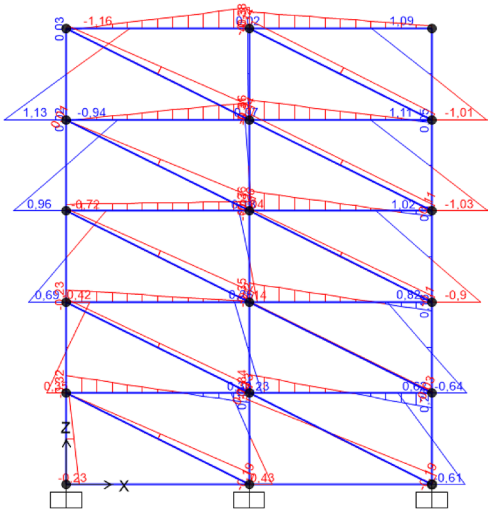

(l) Max. = 1.03 kNm

Figure 23: Continued

Maximum normal stress = 19.41 N/mm^2

Localization: YZ Plane – X = 12 m

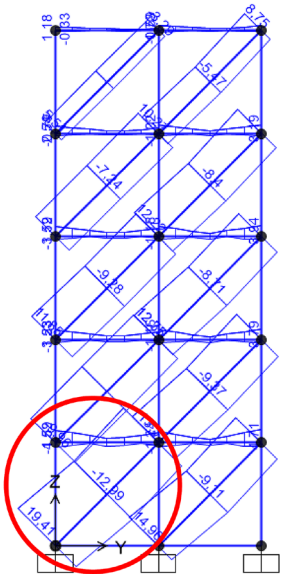

Maximum shear stress = 0.70 N/mm^2

Localization: YZ Plane – X = 12 m

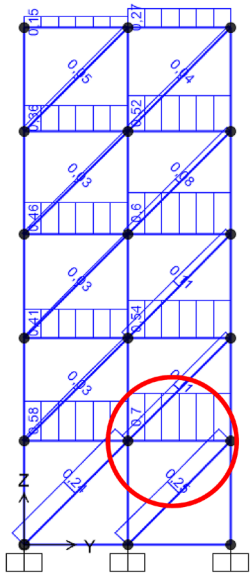

Figure 24: Envelope of maximum/minimum stresses in the modified system. Earthquake in the Y direction.

YZ Plane – X = 0

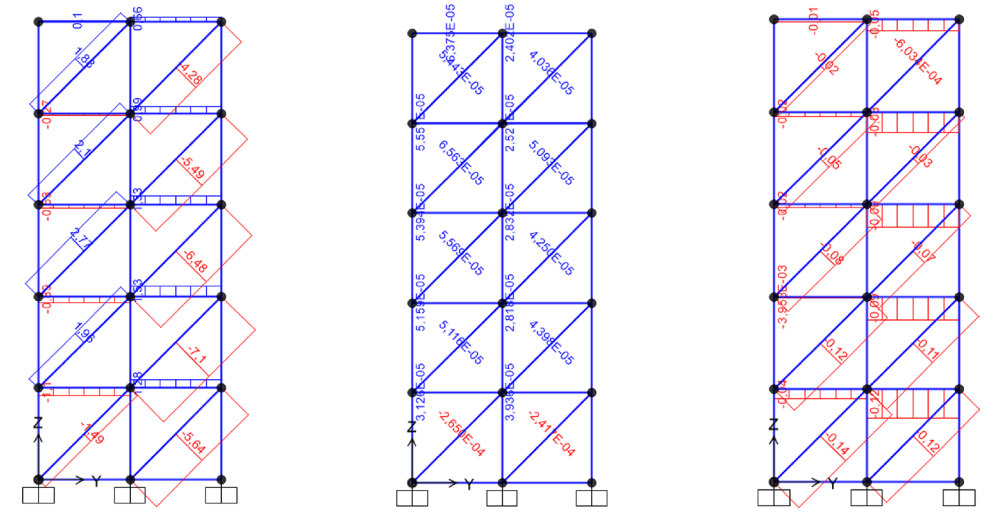

(a) Max. = 7.10 kN (b) Not relevant (c) Max. = 0.14 kN

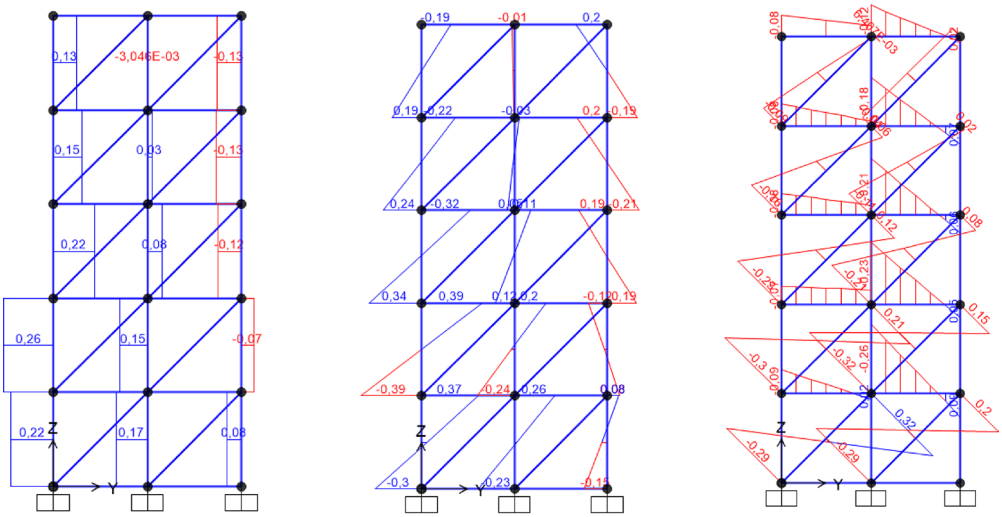

(d) Max. = 0.26 kN (e) Max. = 0.39 kNm (f) Max. = 0.32 kNm

XZ Plane – Y = 0

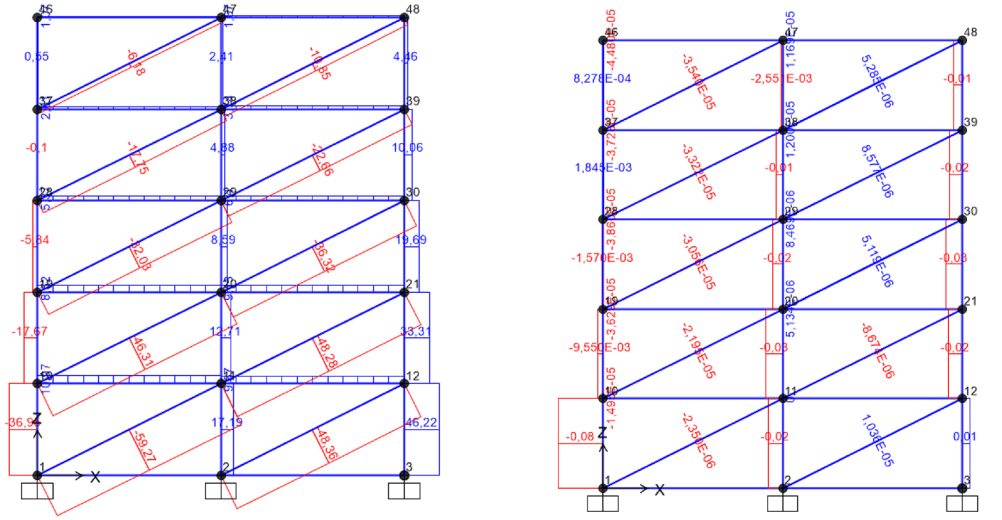

(g) Max. = 59.27 kN (h) Max. = 0.08 kNm

Figure 25: Forces in the building of the original system. Time step 0.66 seconds. Earthquake in the X direction: (a) and (g) Axial force; (b) and (h) Torsion moment; (c) and (i) Shear force in the vertical direction; (d) and (j) Shear force in the horizontal direction; (e) and (k) Bending moment flexing the vertical direction; (f) and (l) Bending moment flexing the horizontal direction.

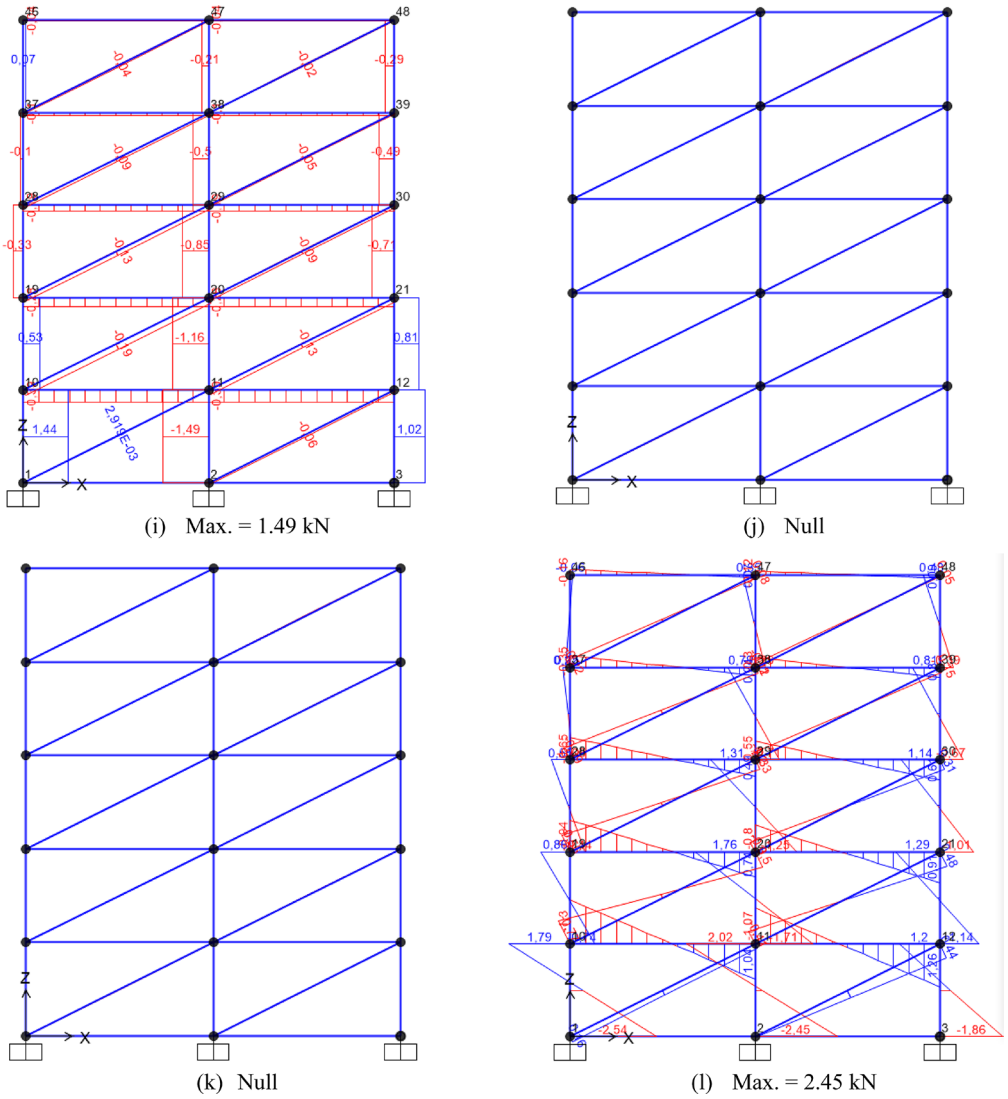

(i) Max. = 1.49 kN (j) Null

(k) Null (l) Max. = 2.45 kN

Figure 25: Continued

The structure movements under earthquake conditions after applying springs are compatible with those presented in **Figure 7** (values according **Table 4**). It can be noted in **Table 4** that the variation of displacements increases from up to down along the building height. Eventually, negative results indicate values superjacent to the previously obtained and presented in **Table 2**. Extreme values occur when an earthquake acts in the Y direction instead of the X direction. Additionally to the previous examination, **Figure 13** and **Figure 14** show the time series of displacements of the reference joints for the Y and X directions when the building is influenced by the earthquake excitation. Judging by the presence of peaks, it is possible to presume the existence of local resonant regimes when the earthquake mobilizes the structure's primary movements. Displacements of the reference joints with respect to the primary and secondary movements are comparatively shown in **Figure 15**. Structural responses in frequency domain considering the original and modified systems are presented from **Figure 16** to **Figure 19**. For defining the dominant frequency, the highest Normalized Amplitude of the FFT was considered.

4.2. Forces and stress analysis

The analysis of forces includes the assessment of axial forces, the torsion moment, shear forces, and bending moments induced on the building sections given in **Figure 7**. The evaluation considers the original and modified systems when submitted to earthquake acting unidirectionally in the Y and X sense. It is important to mention that the effect of an earthquake can produce reflexes in a different direction than the one it acts upon. Because of that motivation, forces to YZ and XZ planes containing the same reference joint are assessed, and the most stressed elements in any position of the structure are verified.

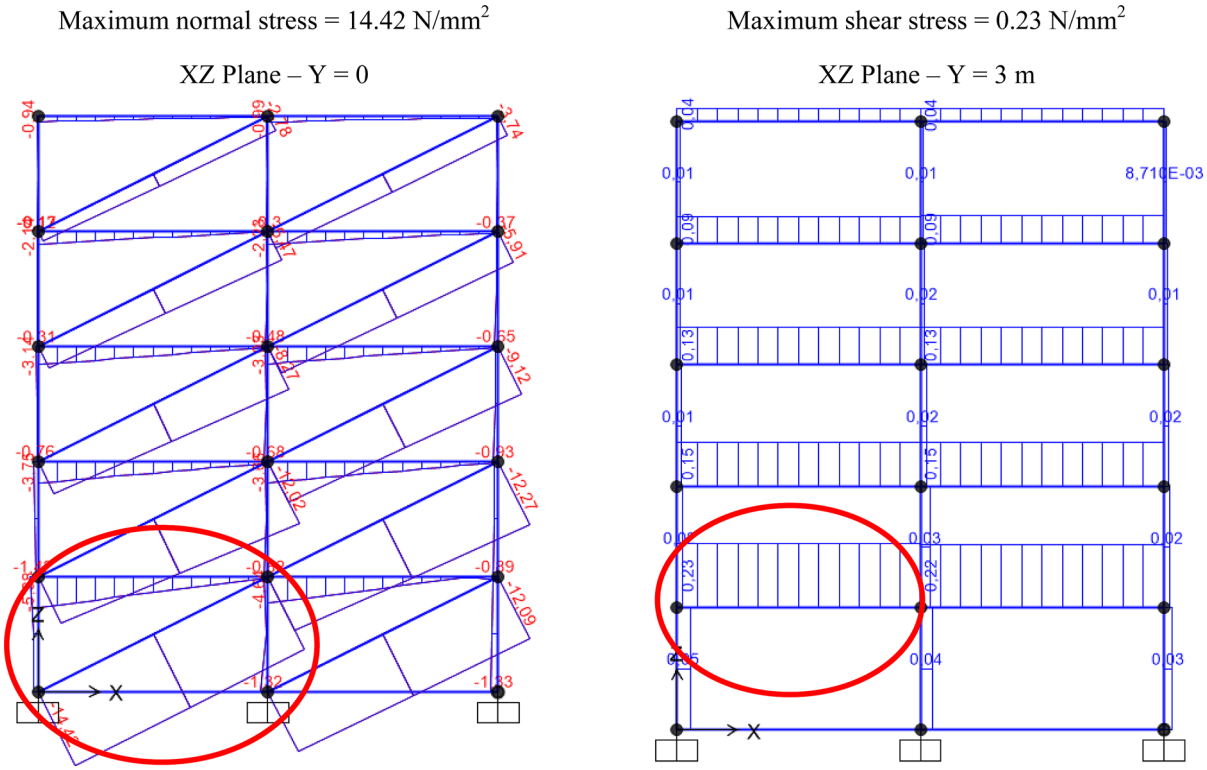

Figure 26: Envelope of maximum/minimum stresses in the original system. Earthquake acting in the X direction.

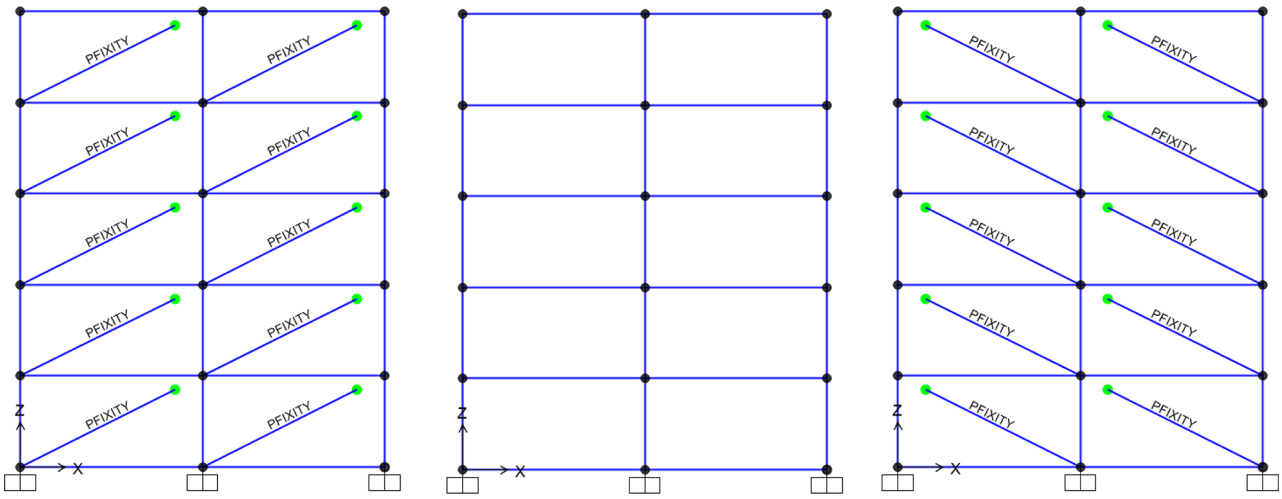

(a) XZ Plane – Y = 0 m (b) XZ Plane – X = 3 m (c) XZ Plane – X = 6 m

Figure 27: Modified system by applying springs to diagonal contained in the XZ planes

4.2.1. Earthquake acting in Y direction

The forces acting on the buildings for an earthquake acting in the Y direction are indicated next as the original as the modified systems at the time step of maximum displacements are presented next.

4.2.1.1.Original system

The maximum normal and shear stresses can be seen in **Figure 21**.

4.2.1.2. Modified system

The first modified system taken in consideration consists of springs applied to diagonals contained in the perimetry of the YZ planes, as shown in **Figure 22**.

The forces indicated in **Figure 23** were obtained for an earthquake acting in the Y direction considering the modified system as described previously.

By observing the entire structure, it is possible to assess the maximum stresses induced in a frame element considering all the set of actuating forces, as shown in

Figure 24, when the earthquake action is according to the Y direction of the building.

4.2.2. Earthquake acting in X direction

4.2.2.1. Original system

The forces induced in the original system regard an earthquake actuating in the X direction are indicated in **Figure 25**.

The maximum normal and shear stresses are presented in **Figure 26**.

4.2.2.2. Modified system

The second modified system consists of springs applied to diagonals contained in the perimetric YZ planes, as shown in **Figure 27**.

The forces in the modified system with an earthquake actuating in the X direction are presented in **Figure 28**. The extreme normal and shear stresses can be seen in **Figure 29**.

All the obtained results for the extreme stresses are summarized in **Table 5**. By assessing the obtained results, it is possible to see that the most stressed elements are concentrated near the ground, first and second floors, although the top of the building presents the largest displacements.

It is also important to register that due to the symmetry of the problem, forces and stresses can be noted with small numerical differences in other frame elements. Considering the steel-yielding stress equal to 250 Mpa, none of the maximum values found for the normal and shear stresses can take the yielding of the material. Applying springs to the structure, there is no significant

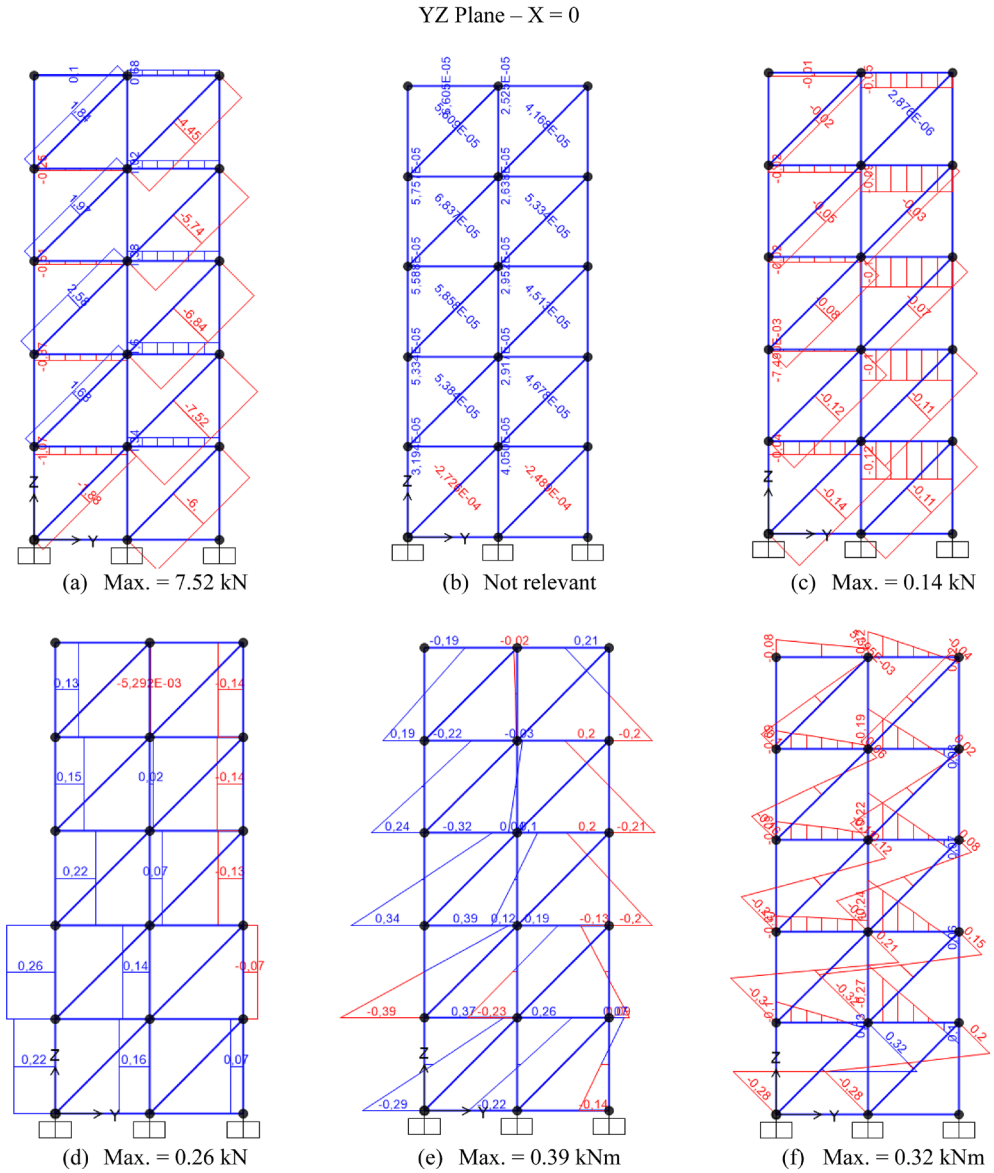

Figure 28: Forces in the building section of the modified system. Time step 0.66 seconds. Earthquake in the X direction: (a) and (g) Axial force; (b) and (h) Torsion moment; (c) and (i) Shear force in the vertical direction; (d) and (j) Shear force in the horizontal direction; (e) and (k) Bending moment flexing the vertical direction; (f) and (l) Bending moment flexing the horizontal direction.

XZ Plane – Y = 0

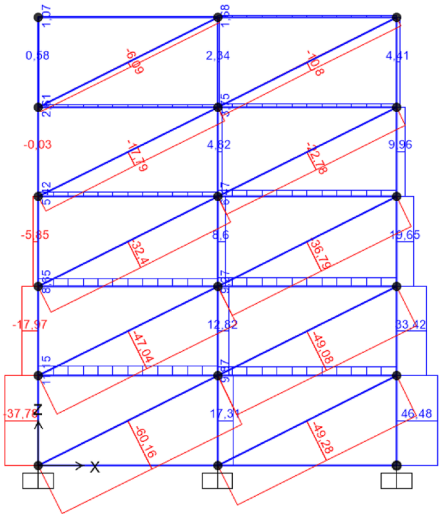

(g) Max. = 60.16 kN

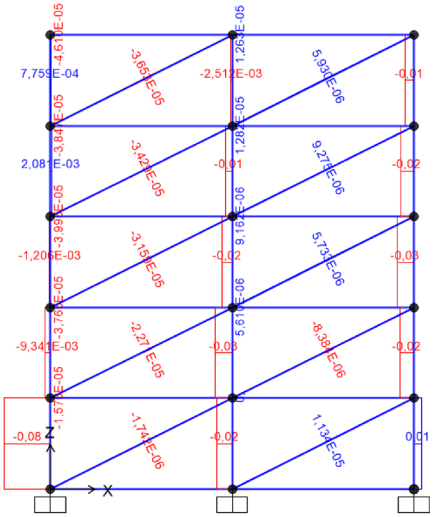

(h) Max. = 0.08 kNm

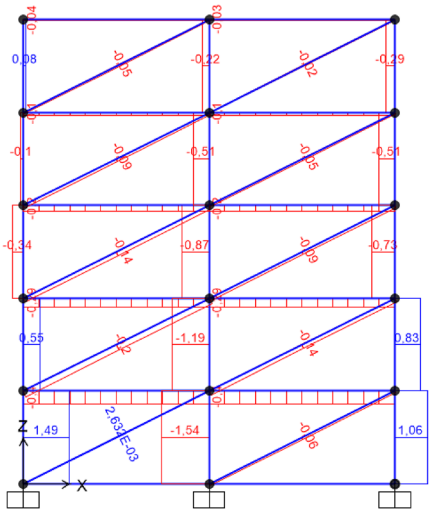

(i) Max. = 1.54 kN

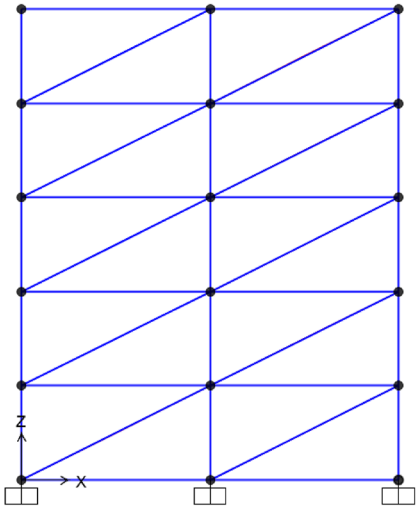

(j) Null

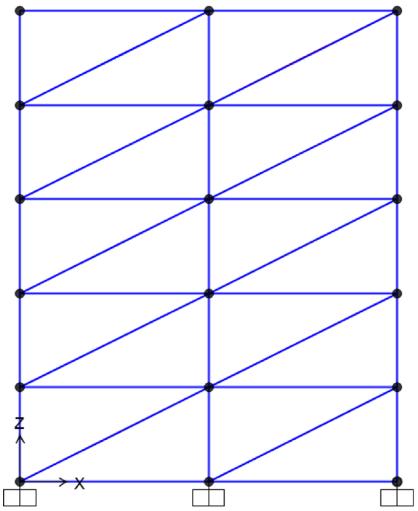

(k) Null

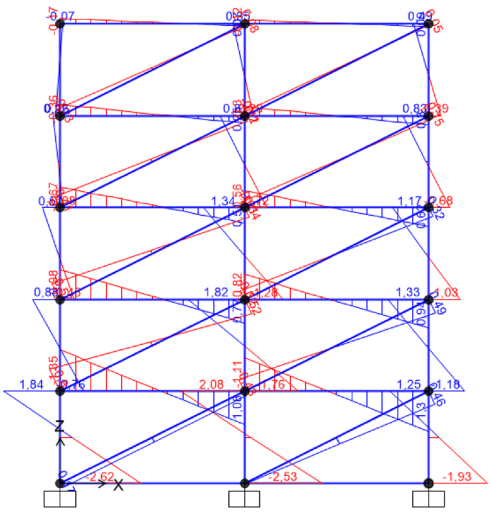

(l) Max. = 2.53 kN

Figure 28: Continued

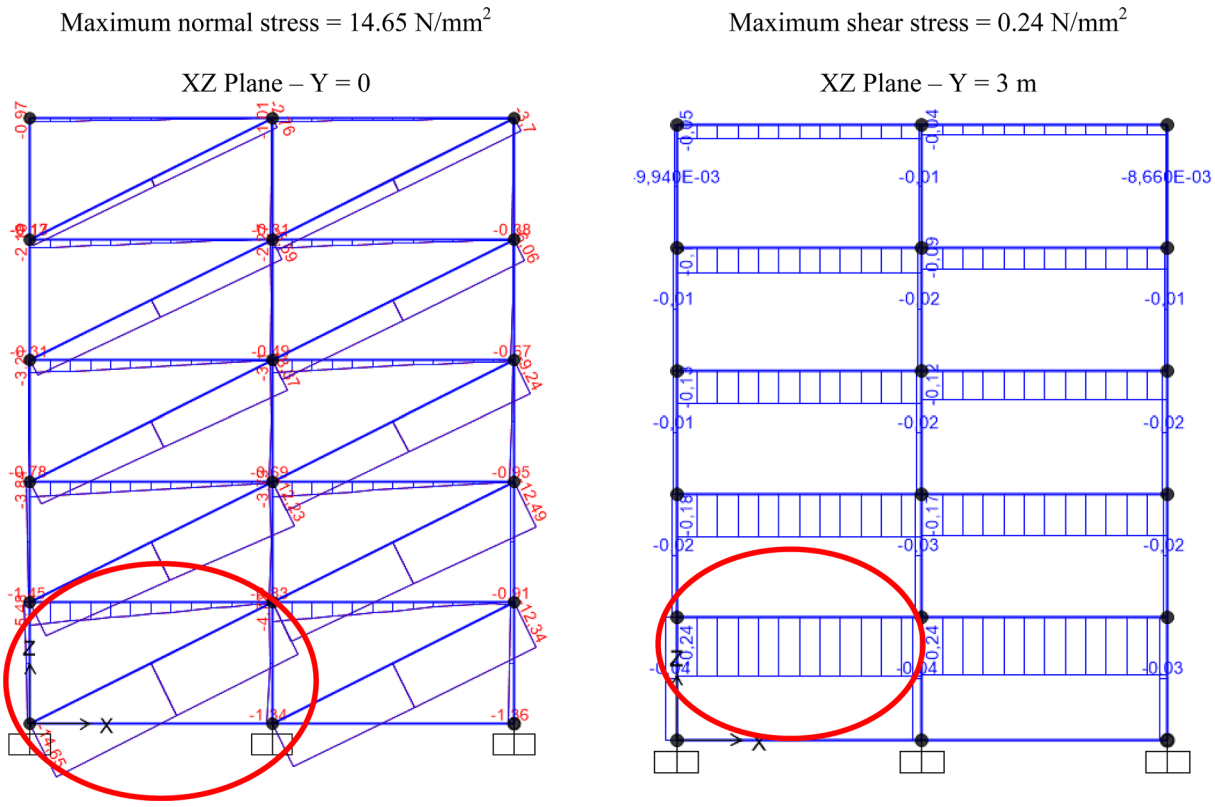

Figure 29: Envelope of maximum/minimum stresses in the modified system. Earthquake acting in the X direction.

change in the induced stresses. As registered by **Mele et al (2019)** an analysis based on strength is an adequate criterium for building with an aspect ratio inferior to 4.

5. Conclusions

A computer simulation based on the finite element method demonstrates the feasibility of using mechanical control devices on the response of a building under seismic action. In this sense, it could be observed that the position of the structure that presented the highest displacements during a simulated seismic event had its vibration frequency relatively adjusted after the insertion of a control system based on the concept of variable stiffness springs.

These springs could have their coefficients calibrated to approximate the vibration frequencies of the building during a seismic action to that of its two first natural vibration modes. Concerning the first mode, the adopted spring led the system to have a frequency that differs by only 1.09% from the original value. About the second one, this difference was 2.87%. The first mode of vibration is associated with the building's planes being more flexible (transversal direction), while the second mode belongs to the direction with the greatest stiffness (longitudinal direction). So, the maximum displacement observed under the earthquake action for the longitudinal direction represents 59% of the transversal direction, when both are primary movements. Relating secondary with primary movements of distinct seismic actions in the building's Y and X directions, the found percentages are 15% and 33%. This means that the seismic activity can't produce a significant effect on the secondary movements as the primary ones. In the field of stress analysis, it is possible to assess that steel yielding does not occur.

Given the dynamic nature of the loading caused by earthquakes, the use of springs can be an efficient tool in modulating the amplitude of displacements and adjusting the vibration frequencies induced by a seismic event. However, the efficiency of a control system is conditioned to the building geometry. High spring coefficient values applied to flexible planes can't produce the desired effect because it is no longer possible to increase the connection's stiffness sufficiently, although being possible to reduce it by diminishing the spring coefficient values. On the other hand, if the spring coefficient assigned to a diagonal is reduced, the structural frequency decreases. If this is important for a specific analysis, an eventual resonance with an earthquake excitation can be avoided.

Thus, it is possible to conclude that the use of variable stiffness springs as elements of vibration control and mitigation of the effects of seismic concussions becomes a viable strategy if the goal is to keep the natural frequencies as close as possible to their original values during seismic activity. Displacements can be controlled as well. Eventually, studies on other vibration modes are expected in future work as well as analyses of buildings

with higher aspect ratios and with different structural arrangements.

Acknowledgements

The authors thank the National Council for Scientific and Technological Development (CNPq) for the given support in the form of research grants.

References

Banerji, P., and Samanta, A. (2011): Earthquake vibration control of structures using hybrid mass liquid damper. Engineering structures, 33(4), 1291-1301. https://doi.org/10.1016/j.engstruct.2011.01.006

Bauchau, O.A., Craig, J.I. (2009). Euler-Bernoulli beam theory, Structural Analysis, Solid Mechanics and its Applications, Vol. 163. Springer, Dordrecht. https://doi.org/10.1007/978-90-481-2516-6_5

Beneveli, S.M.A. (2002): Hybrid control for vibration attenuation in buildings. Pontifical Catholic University of Rio de Janeiro, Rio de Janeiro, Doctoral Thesis, Graduate Program in Civil Engineering (*in Portuguese with abstract in English*). https://doi.org/10.17771/PUCRio.acad.3124

Bigdeli, Y., and Kim, D. (2016): Damping effects of the passive control devices on structural vibration control: TMD, TLC and TLCD for varying total masses. KSCE Journal of Civil Engineering, 20, 301–308. https://doi.org/10.1007/s12205-015-0365-5

Brazilian Association of Technical Standards, ABNT NBR 15421 (2006): Design of earthquake-resistant structures - Procedure, Rio de Janeiro (*in Portuguese*).

Campos, J.E.G., Xavier, T.O., and Freitas-Silva, F.H. (2016): Records of neotectonics activity in the Federal District. Geosciences. São Paulo, UNESP, 35, 2, 203–219 (*in Portuguese with abstract in English*). https://ppegeo.igc.usp.br/index.php/GEOSP/article/view/9019

Dantas, G.L.J., Menezes, C.M., Pacheco, C.V., and Wahrhaftig, A.M. (2021): Springs with proportional stiffness to the applied force. In: Proceedings of the 26th International Congress of Mechanical Engineering. Rio de Janeiro, Brazil: ABCM. https://doi.org/10.26678/ABCM.COBEM2021.COB2021-0024

Davenport, A.G. (1961): The spectrum of horizontal gustiness near the ground in high winds. Quarterly Journal of the Royal Meteorological Society. https://doi.org/10.1002/qj.49708737208

Duffin, R.J. (1969): The Influence of Poisson's Ratio on the Vibrational Spectrum. SIAM – Journal on Applied Mathematics, 17(1), 179–191. https://www.jstor.org/stable/2099252

García, W.E., and Galeano, I.D.O. (2018): Solution of high velocity anomalies imperceptible to the seismic resolution, by means of synthetic models, Penobscot Field, Canada. Rudarsko-geološko-Naftni Zbornik, 34(1). https://doi.org/10.17794/rgn.2019.1.7

Gómez, A.L.Z. (2007): Vibration control in buildings subjected to the action of dynamic loads using mass damper tuning in the form of pendulum. University of Brasília, Brasília, Dissertation, Master in Structures and Civil Construction (*in Portuguese with abstract in English*). https://repositorio.unb.br/handle/10482/2287Gupta, A., and Pradyumna, S. (2022): Geometrically nonlinear dynamic analysis of variable stiffness composite laminated and sandwich shell panels. Thin-Walled Structures, 173, 109021. https://doi.org/10.1016/j.tws.2022.109021

Hadi, M.N.S., and Arfiadi, Y. (1998): Optimum Design of Absorber for MDOF Structures. Journal of Structural Engineering, 124(11), 1272-1280. https://doi.org/10.1061/(ASCE)0733-9445(1998)124:11(1272)

Hwang, J.-S., Kim, J., Kim, and Y.-M. (2017): Rotational inertia dampers with toggle bracing for vibration control of a building structure. Engineering Structures, 29(6), 1201–1208. https://doi.org/10.1016/j.engstruct.2006.08.005

Ikeda, Y. (2009): Active and semi-active vibration control of buildings in Japan – Practical applications and verification. Structural Control and Health Monitoring, 16(7-8), 703–723. https://doi.org/10.1002/stc.315

Jaya Syahbana, A., Iqbal, P., Irsyam, M., Asrurifak, M., and Hendriyawan, H. (2021): Smoothed Gridded Seismicity Effect for Land-Use Development, Case Study: Kalimantan Island, Indonesia. Rudarsko-geološko-Naftni Zbornik, 36(3). https://doi.org/10.17794/rgn.2021.3.8

Krylov V.V. (1995): Generation of Low-Frequency Ground Vibrations by Sound Waves Propagating in Underground Gas Pipes. Journal of Low Frequency Noise, Vibration and Active Control, 14(3):143–149. https://doi.org/10.1177/026309239501400303

Laura, P.A.A., Sonzogni, V., and Romanelli, E. (1996): Effect of Poisson's ratio on the fundamental frequency of transverse vibration and buckling load of circular plates with variable profile. Applied Acoustics, 47(3), 263–273. https://doi.org/10.1016/0003-682X(95)00053-C

Li, Z., Chen, W., Zhang, J., Li, Q., Wang, J., Fang, Z., and Yang, G. (2022): A novel cable-driven antagonistic joint designed with variable stiffness mechanisms. Mechanism and Machine Theory, 171, 104716. https://doi.org/10.1016/j.mechmachtheory.2021.104716

Lin, H.-P. (2004): Direct and inverse methods on free vibration analysis of simply supported beams with a crack. Engineering Structures, 26(4), 427–436. https://doi.org/10.1016/j.engstruct.2003.10.014

Liu, H., Zhu, D., and Xiao, J. (2020): Conceptual design and parameter optimization of a variable stiffness mechanism for producing constant output forces. Mechanism and Machine Theory, 154, 104033. https://doi.org/10.1016/j.mechmachtheory.2020.104033

Loh, C.H., and Chao, C.H. (1996): Effectiveness of active tuned mass damper and seismic isolation on vibration control of multi-storey building. Journal of Sound and Vibration 193(4), 773–792. https://doi.org/10.1006/jsvi.1996.0315

Magalhães, K.M.M, Wahrhaftig, A.M, and Brasil, R.M.L.R.F (2023): Strain regime induced by axial compression in slender reinforced concrete columns using different mathematical approaches. Structures, 49, 655–665. https://doi.org/10.1016/j.istruc.2023.01.148

Magalhães, K.M.M., Brasil, R.M.L.R.F., Wahrhaftig, A.M., Siqueira, G.H., Bondarenko, I., and Neduzha, L. (2022):

Influence of atmospheric humidity on the critical buckling load of reinforced concrete columns. International Journal of Structural Stability and Dynamics, 22(01), 2250011. https://doi.org/10.1142/S0219455422500110

Mahato, A.C., Ghoshal, S.K., and Samantaray, A.K. (2019): Influence of variable inertia flywheel and soft switching on a power hydraulic system. SN Applied Sciences, 1, 605. https://doi.org/10.1007/s42452-019-0623-0

Mele, E., Imbimbo, M., and Tomei, V. (2019): The effect of slenderness on the design of diagrid structures. International Journal of High-Rise Buildings, 8(2), 83–94. https://doi.org/10.21022/IJHRB.2019.8.2.83

Mirfakhraei, S.F., Andalib, G., and Chan, R. (2019): Active scissor-jack for seismic risk mitigation of building structures. SN Applied Sciences, 1, 191. https://doi.org/10.1007/s42452-019-0210-4

Moomivand, H., Moosazadeh, S., and Gilani, S.-O. (2022): A new empirical approach to estimate the ratio of horizontal to vertical in-situ stress and evaluation of its effect on the stability analysis of underground spaces. Rudarsko-geološko-Naftni Zbornik, 37(3), 97–107. https://doi.org/10.17794/rgn.2022.3.8

Moutinho, C.M.R. (2007): Vibration control in civil engineering structures. Doctoral thesis, Faculty of Engineering, University of Porto, Porto, Portugal (*in Portuguese with abstract in English*). http://hdl.handle.net/10216/11186

Murawski, K. (2022): Technical lateral buckling with stress and strain analysis of semi-slender thin-walled cylindrical pinned column simplified with A= Ael, Jz= Jzel and Epl = Ec. Scholar Freedom. https://doi.org/10.54769/9UYHEQ2AF6

Murawski, K., and Wahrhaftig, A.M. (2021): Stability, Stress and strain analysis of very slender pinned thin-walled box columns according to FEM, Euler and TSTh. American Journal of Engineering and Applied Sciences, 14(2), 214–257. https://doi.org/10.3844/ajeassp.2021.214.257

Palermo, M., Silvestri, S., Gasparini, G., Trombetti, T. (2015): Crescent shaped braces for the seismic design of building structures. Materials and Structures, 48, 1485–1502. https://doi.org/10.1617/s11527-014-0249-z

Pradhan, B.R., Kakkar, S.S., and Saxena, A.P. (1969): Variation of modulus of elasticity with frequency of vibration. Indian Journal of Physics, 43, 468-473. https://core.ac.uk/download/pdf/93519563.pdf

Preve, W.S., D'Espindula, G.P.C., and Valdati, J. (2017): Moderate seismic shocks in Brazil: a survey of events recorded in the 20th and 21st centuries and the dissemination of preventive measures. In: XVII Brazilian Symposium on Applied Physical Geography, Campinas/SP. The challenges of physical geography on the frontier of knowledge, 1, 3928–3940 (*in Portuguese*). https://doi.org/10.20396/sbgfa.v1i2017.2542

Rose, T.A., Smith, P.D., May, J.H. (2006): The interaction of oblique blast waves with buildings. Shock Waves 16, 35–44. https://doi.org/10.1007/s00193-006-0051-0

Sabelli, R., Mahin, S., Chang, C. (2003): Seismic demands on steel braced frame buildings with buckling-restrained braces. Engineering Structures, 25(5), 655–666. https://doi.org/10.1016/S0141-0296(02)00175-X

SAP2000 (2017): Analysis reference manual. Integrated software for structural analysis and design. Computers and Structures, Inc. Berkeley, California. https://www.csiamerica.com/Seeber, L., and Armbruster, J.G. (1988): Seismicity along the Atlantic seaboard of the U.S.: intraplate neotectonics and earthquake hazard. In: The Atlantic Continental Margin: U.S.. The Geology of North America. R.E. Sheridan & J.A. Grow (eds.), Geological Society of America, Boulder, 565–582. https://doi.org/10.1130/DNAG-GNA-I2.565

Sharma, N., Swain, Prasant, K., Maiti, D.K., and Singh, B.N. (2022): Static and free vibration analyses and dynamic control of smart variable stiffness laminated composite plate with delamination. Composite Structures, 280, 114793. https://doi.org/10.1016/j.compstruct.2021.114793

Silva M.A., Wahrhaftig, A.M., Brasil, R.M. (2021): Remarks on optimization of impact damping for a non-ideal and nonlinear structural system. Journal of Low Frequency Noise, Vibration and Active Control, 40(2), 948–965. https://doi.org.10.1177/1461348420940074

Singh, T., Kalra M., Misra, A. K. (2020): Simplified probabilistic seismic assessment of dampers in tall and braced structures in buildings. Journal of Engineering, Design and Technology, 18(5), 1037–1052. https://doi.org.10.1108/JEDT-09-2019-0234

Smith, P. D., Rose, T. A, Saotonglang, E., Conwep (1999): Clearing of blast waves from building facades. Proceedings of the Institution of Civil Engineers - Structures and Buildings, 134(2), 193–199. https://doi.org/10.1680/istbu.1999.31385

Tanaka, M., Ikeda, K., Fujii, F. (2023): Versatile benchmark model reproducing snap-through, asymmetric, symmetric unstable/stable, and multiple bifurcation including hill-top branching in structural instability. Computer Methods in Applied Mechanics and Engineering, 403, Part B, 115719. https://doi.org/10.1016/j.cma.2022.115719

Tavares, A.C., Montenegro, C.G.L, Bezerra, F.H.R., Ferreira, J.M., and Sousa, M.O.L. (2013): Map of neotectonic faults of Borborema Province based on seismological, geophysical, and geological data. In: 13th International Congress of the Brazilian Geophysical Society. Rio de Janeiro, Brazil, 1993–1997 (*in Portuguese with abstract in English*). https://doi.org/10.1190/sbgf2013-409

Valencia, L.A.L., González, Y.V., and Zambrano, D.M.B. (2022): Study of a semi-active control system to reduce lateral displacement in framed structures under seismic load. Ingeniería e Investigación, 42(3), e85937, 85937-85937. https://doi.org/10.15446/ing.investig.85937

Van Loon, A.J., Pisarska-Jamroży, M., and Woronko, B. (2020): Sedimentological distinction in glacigenic sediments between load casts induced by periglacial processes from those induced by seismic shocks. Geological Quarterly, 64(3):626–640. http://dx.doi.org/10.7306/gq.1546

Ventsel, E., Krauthammer, T., and Carrera, E. (2002): Thin Plates and Shells: Theory, Analysis and Applications. Applied Mechanics Reviews, 55(4), B72-B73. https://doi.org/10.1115/1.1483356Vibrationdata. Time History Data Files from El Centro Site Imperial Valley Irrigation Dis-

trict, Nort-South Component. http://www.vibrationdata.com/elcentro.htm. Accessed Dec.22, 2022.

Wahrhaftig, A.d.M., Magalhães, K.M.M., Brasil, R.M.L.R.F., Murawski, K. (2021): Evaluation of mathematical solutions for the determination of buckling of columns under self-weight. Journal of Vibration Engineering & Technologies, 9, 733–749. https://doi.org/10.1007/s42417-020-00258-7

Wahrhaftig, A.M. (2020): Time-dependent analysis of slender, tapered reinforced concrete columns. Steel and Composite Structures, 36, 2, 229–247. https://doi.org/10.12989/scs.2020.36.2.229

Wahrhaftig, A.M., Dantas, J.G.L., Brazil, R.M.L.R.F., and Kloda, L. (2022): Control of the vibration of simply supported beams by using springs with proportional stiffness to the axially applied force. Journal of Vibration Engineering & Technologies, 10, 2163–2177. https://doi.org/10.1007/s42417-022-00502-2

Wahrhaftig, A.M., Silva, M.A. (2017): Using computational fluid dynamics to improve the drag coefficient estimates for tall buildings under wind loading. The Structural Design of Tall and Special Buildings, 27, 3, e1442. https://doi.org/10.1002/tal.1442

Wu, S., He, H., Cheng, S., and Chen, Y. (2021): Story stiffness optimization of frame subjected to earthquake under uniform displacement criterion. Structural and Multidisciplinary Optimization 63(3), 1533–1546. https://doi.org/10.1007/s00158-020-02761-7

Xu, X.-J., and Deng, Z.-C. (2016): Closed-form frequency solutions for simplified strain gradient beams with higher-order inertia, European Journal of Mechanics - A/Solids, 56, 59–72. https://doi.org/10.1016/j.euromechsol.2015.10.005

Yari, M., Ghadyani, D., and Jamali, S. (2022): Development of a 3D numerical model for simulating a blast wave propagation system considering the position of the blasting hole and in-situ discontinuities. Rudarsko-geološko-Naftni Zbornik, 37(2), 67–78. https://doi.org/10.17794/rgn.2022.2.6

Zhan, M., Liu, J., Chen, X., Lizhen Zhang, Wang, S., and Li, T. (2022): Seismic response control of T-shaped porcelain column circuit breaker based on shape memory alloy cables. Journal of Vibration Engineering & Technologies, 10, 2313–2326. https://doi.org/10.1007/s42417-022-00568-y

Zhang, B., Billings, S.A., Lang, Z.Q., and Tomlinson, G.R. (2009): Suppressing resonant vibrations using nonlinear springs and dampers. Journal of Vibration and Control, 15, 11, 1731–1744. https://doi.org/10.1177/1077546309102668

Zhou, K, and Li, Q.-S. (2022): Modal identification of high-rise buildings under earthquake excitations via an improved subspace methodology. Journal of Building Engineering, 52(15 July), 104373. https://doi.org/10.1016/j.jobe.2022.104373

SAŽETAK

Opruge promjenjive krutosti u kontroli seizmičkih djelovanja u zgradama

Mnoge regije u svijetu imaju iskustva s geohazardima i potresima. Kontrola vibracija uzrokovanih potresima na zgradama jedan je od velikih izazova u seizmičkim regijama, budući da mogu uzrokovati strukturnu, materijalnu i osobnu štetu, te se moraju uzeti u obzir s posebnom pozornošću prilikom projekata gradnje. Iz tog razloga potrebno je maksimalno umanjiti štetne učinke potresa na građevine. Ova studija nastoji procijeniti, kroz teoriju mehaničkih vibracija, primjenu opruga promjenjive krutosti u kontroli ubrzanja izazvanih seizmičkim djelovanjem, budući da ova vrsta opruga uvodi restorativne sile u sustav. Evaluacija modela je provedena numeričkom simulacijom metodom konačnih elemenata. U modeliranju je korištena okvirna konstrukcija idealizirane građevine, gdje su stupovi i grede prikazani linijskim elementima, a podovi površinskim elementima. U simulaciji, opruge promjenjive krutosti umetnute su u čvorove kako bi se kontrolirale vibracije uzrokovane potresima. Ti su uređaji dodani strukturi građevine na različitim visinama i u različitim smjerovima, s ciljem da se ponašanje strukture održi nepromijenjenim, neutralizirajući učinke potresa. Na temelju rezultata istraživanja moguće je definirati optimalnu krutost i položaje u koji moraju biti postavljene opruge kako bi se postigla stabilnost konstrukcije tijekom djelovanja potresa.

Ključne riječi:
opružni nosači; promjenjiva krutost; seizmičko djelovanje; numerička simulacija; strukturalne vibracije

Author's contribution

Alexandre Wahrhaftig (1) (Associate Professor, PhD., Civil Engineering) conceived the problem, supervised the analysis, helped the data interpretation and presentation of results, and harmonized the final version of the text. **Julia Dantas (2)** (Researcher of the Institutional Scientific Initiation Program (PIBIC/UFBA-CNPq), BSc., Mechanical Engineering) elaborated the computational model, performed the seismic analyses, generated results, and helped to write the text. **Cibele Menezes (3)** (MSc. Candidate, Civil Engineering) contributed to writing the text and literature review, and the discussion of the results. **Larysa Neduzha (4)** (Professor, PhD., Civil Engineering) contributed to the literature review, discussed technical issues, contributed to the text, and checked formatting requirements.